High-current electric-discharge light sources

A. F. Aleksandrov and A. A. Rukhadze

M. V. Lomonosov Moscow State University;
P. N. Lebedev Physics Institute, Academy of Sciences of the USSR.
Usp. Fiz. Nauk 112, 193-230 (February 1974).

This review presents systematically the results of investigations of the physics of high-current discharges in dense low-temperature plasmas and it is based, to a considerable extent, on the results of theoretical and experimental investigations carried out since 1967 at the Lebedev Physics Institute and in the Physics Department of the Moscow State University. The prime aim of these investigations was to determine the possibility of using high-current discharges in dense plasmas as radiation sources for the pumping of modern high-power lasers. It was found that the physics of high-current light-emitting discharges went well beyond the utilitarian task of providing high-power light sources, and covered little known branches of the physics of dense plasmas at relatively low temperatures, when the radiation dominated the energy balance and transfer processes. This general approach to the physics of plasmas is adopted in the present review. It comprises a theoretical part (Chap. I), which deals with the results of theoretical analyses of the formation, equilibrium, and stability of plasmas in high-current light-emitting discharges, and a part (Chap. II) which gives the results of an experimental investigation of the physical processes in such discharges and analyzes their characteristics as light sources. The review is intended for physicists and engineers investigating high-power light sources, magnetohydrodynamics, and physics of dense low-temperature plasmas. The review covers papers which appeared up to the beginning of 1973.

CONTENTS

1. Introduction 44
I. Equilibrium, Stability, and Formation of Light-Emitting Discharges 45
II. Experimental Investigations of High-Current Light-Emitting Discharges 52
III. Conclusions 60
Literature 61

1. Introduction

Electric discharges in gases have been used for a long time as light sources in various branches of science and technology. The most widely used sources are the xenon lamps,[1,2] which utilize low-current arc discharges at low pressures. We shall define low-current discharges as those in which a conducting ionized gas (plasma) is not confined by the magnetic field of the discharge current and, therefore, the gas is in direct contact with the walls of the discharge enclosure. The intensity of such low-current electric-discharge light sources is not very high because of this contact between the plasma and the enclosure walls; this intensity does not usually exceed that of a black body kept at a temperature $T \approx 1-1.5$ eV.

In view of the rising demands of science and technology for high-intensity light sources, the research effort has shifted since the 1950's to high-current pulse discharges in which plasmas are held in equilibrium by the magnetic field of the discharge current. A suitable selection of the composition of a discharge plasma, its density, discharge configuration, and electric circuit parameters can ensure conditions favorable for the almost total conversion of the stored electrical energy into the radiation energy. The results of the early investigations of high-current discharges as light sources can be found in review papers.[3,4] However these investigations have been mostly experimental and the powers concerned have been low. Systematic studies of the physics of powerful high-current discharges under conditions suitable for their use as intensive light sources have begun only recently when the efficiency of such discharges in laser pumping was demonstrated in [5]. The high-current discharges are particularly promising as sources of ultraviolet or shorter-wavelength radiation. Apart from their application as pumping sources for various types of laser, high-power pulse light sources have a wide range of application such as the chemistry of flash photolysis [6] and in other branches of science and technology.

The radiation sources suitable for the pumping of high-power lasers should have the following principal characteristics: the effective temperature of the source, corresponding to the temperature of the radiating surface of an absolute black body, should be $T \approx 2-10$ eV and the duration of the radiation pulses should be $\tau = 30-100$ μsec. Obviously, a dense plasma with a total charged-particle concentration $N_t \geq 10^{18}$ cm^{-3} can be maintained for this relatively long time at such high temperatures only by a continuous ohmic heating of a strong discharge current, which should also

be capable of magnetic compression of the discharge plasma (pinch effect).

High-current self-pinched discharges were first considered theoretically by Bennett[7] and then in the 1950's they were studied in detail in many theoretical and experimental papers (a detailed bibliography can be found in monographs [8,9])[1)] with the aim of generating a high-temperature plasma suitable for controlled thermonuclear fusion. Experiments indicated that a high-temperature self-pinched discharge could exist only for several microseconds; after this period, such a discharge became highly unstable and broke up. This behavior of the self-pinched discharge in a high-temperature plasma was later explained in the theoretical papers of several workers who developed a magnetohydrodynamic theory of the stability of such discharges.[12] However, strictly speaking, this theory cannot be applied to the physical processes in radiating discharges of interest to us since thermonuclear investigations are concerned with a not very dense optically transparent high-temperature plasma under conditions such that the radiation does not dominate the dynamics and energy balance in the discharge, whereas the discharges suitable as light sources occur in an optically dense plasma whose temperature is relatively low. In such a plasma the radiation plays the dominant role in the development of the discharge. Moreover, the effects due to the finite conductivity of the plasma (absence of the skin effect, diffusion of electric and magnetic fields, etc.), which do not play any significant role in high-temperature thermonuclear plasma, become significant in a low-temperature plasma.

The theory of the equilibrium and stability of the high-current self-pinched discharge, allowing for the finite conductivity and influence of radiation, was developed in [13-18] (see also [19-21]). Information on the formation of such discharges in vacuum and in high-pressure gases was reported in [19-26]. Finally, numerical methods for the solution of the magnetohydrodynamic equations, allowing for the influence of radiation, were developed in [27-29] for the problems concerning the formation of a discharge in a dense low-temperature plasma. The results of the first investigations of light-emitting discharges were presented in a review paper at the Ninth International Conference on Phenomena in Ionized Gases held in Bucharest in 1969.[30] Since that time, our knowledge of light-emitting discharges has become much deeper because of further systematic experimental investigations carried out mainly at the P.N. Lebedev Physics Institute of the USSR Academy of Sciences and in the Physics Department of the Moscow State University, as well as because of the refinement of the theoretical representations and improvements in the numerical methods for the analysis of the dynamics of high-current light-emitting discharges.

The purpose of the present review is to present the experimental results obtained in studies of light-emitting discharges of various configurations and to compare them with the current theory. The review consists of two parts. In the first part, we shall briefly present results of theoretical analysis of the equilibrium, stability, and formation of light-emitting discharges in vacuum and in gases. The second part will present an analysis of the experimental results. Conclusions of the review will give briefly the potential applications of light-emitting discharges as high-power light sources and will suggest the optimal parameters of these discharges under various conditions; the directions of further investigations will also be pointed out.

I. EQUILIBRIUM, STABILITY, AND FORMATION OF LIGHT-EMITTING DISCHARGES

2. Basic equations describing plasma dynamics of light-emitting discharges

As mentioned earlier, the discharge parameters (linear dimensions, geometrical configuration, type of gas, density, and temperature) are selected so as to produce the radiation in the required part of the spectrum and of the required duration. Typical parameters of light-emitting discharges are: temperature $T \approx 2-10$ eV, ion density $N \approx 10^{18}-10^{21}$ cm^{-3}, duration $\tau \approx 30-100$ μsec, and linear dimensions (thickness of the current layer) $r_0 \approx 1$ cm. At such temperatures, a discharge plasma is practically completely ionized and its confinement requires magnetic fields (generated by the discharge current) $B = \sqrt{8\pi N\kappa T} \sim 10^4-10^5$ Oe. The mean free path of particles in such a plasma is clearly much shorter than its dimensions or the Larmor radius of the rotation of particles in the magnetic field of the current so that the transport coefficients are isotropic and a local thermodynamic equilibrium (LTE) is established at each point in the course of the discharge. Therefore, in order to describe the dynamics of a plasma of interest to us, we can use the following system of magnetohydrodynamic equations, allowing for the radiation flux:[31]

$$\left.\begin{aligned} &\operatorname{div}\mathbf{B}=0,\quad \operatorname{rot}\mathbf{B}=\frac{4\pi}{c}\sigma\left\{\mathbf{E}+\frac{1}{c}[\mathbf{v},\ \mathbf{B}]\right\},^{2)}\\ &-c\operatorname{rot}\mathbf{E}=\frac{\partial\mathbf{B}}{\partial t}=\operatorname{rot}[\mathbf{v},\ \mathbf{B}]-\frac{c^2}{4\pi}\operatorname{rot}\left(\frac{1}{\sigma}\operatorname{rot}\mathbf{B}\right),\\ &\frac{\partial\rho}{\partial t}+\operatorname{div}\rho\mathbf{v}=0,\\ &\rho\left[\frac{\partial\mathbf{v}}{\partial t}+(\mathbf{v}\nabla)\mathbf{v}\right]=-\nabla P+\frac{1}{4\pi}[\operatorname{rot}\mathbf{B},\ \mathbf{B}],\\ &\frac{\partial}{\partial t}\left(\frac{\rho v^2}{2}+\rho\varepsilon+\frac{B^2}{4\pi}\right)+\operatorname{div}\left[\rho\mathbf{v}\left(\frac{v^2}{2}+\varepsilon+\frac{P}{\rho}\right)\right]=\mathbf{jE}-\operatorname{div}\mathbf{S}, \end{aligned}\right\} \quad (2.1)$$

where $\mathbf{B}$ and $\mathbf{E}$ are the magnetic induction and electric field; $\mathbf{j}$ is the current density; $\mathbf{v}$ is the plasma velocity; ρ is the plasma density; P is the pressure; ϵ is the internal energy; σ is the conductivity of the plasma; $\mathbf{S}$ is the radiation flux vector; c is the velocity of light. In the case of a totally ionized plasma considered in the ideal gas approximation (under the conditions considered by us, such an approximation is well justified[19,20]), we have

$$\left.\begin{aligned} P&=(1+z)\varkappa NT=\frac{(1+z)\rho\varkappa T}{M_i}=v_s^2\rho,\\ \varepsilon&=c_vT=\frac{3}{2}\frac{(1+z)\varkappa T}{M_i}=\frac{3}{2}v_s^2,\\ \sigma&=\frac{\alpha}{z}T^{3/2}, \end{aligned}\right\} \quad (2.2)$$

where M_i is the mass of the plasma ions; z is their effective charge (in the range of parameters of interest to us $z \approx 2-3$); $v_S = \sqrt{(\kappa T/M_i)(1+z)}$ is the velocity of isothermal sound; $\alpha \approx 4\times 10^7$.

The system (2.1) ignores the electronic heat conduction from the plasma compared with the radiative heat flux, and it also ignores the viscosity of the plasma, which is justified by a large margin for the light-emitting parameters mentioned above.[19,20] The radiation flux vector $\mathbf{S}$ is found by solving the transfer equation, namely,[31]

$$\mathbf{S}=\int_0^\infty d\nu\int d\Omega\Omega I_\nu,$$

$$\Omega \nabla I_\nu = \varkappa_\nu (I_{\nu e} - I_\nu)(1 - e^{-h\nu/\varkappa T}). \quad (2.3)$$

Here, I_ν is the spectral density of the radiation intensity emitted into a solid angle Ω, $I_{\nu l} = 2h\nu^3 c^{-2} (e^{h\nu/\varkappa T} - 1)^{-1}$ is the equilibrium radiation intensity; $\varkappa_\nu$ is the absorption coefficient of frequency ν, which is governed by some particular absorption mechanism which predominates under the given conditions (explicit expressions for $\varkappa_\nu$ can be found in [31]).

The greatest interest naturally lies in the discharge conditions such that a given type of absorption of light in the plasma has little influence on the main parameters of the plasma light source. This is true of an optically opaque plasma in which the mean free path of the quanta is less than the typical dimensions of the discharge or, more precisely, when $l_R \ll r_0$, where l_R is the Rosseland range of quanta in a medium. The expressions for l_R applicable to different light-absorption mechanisms are given in [31]. We shall give here the most typical of these expressions, which will be employed later:

$$l_R = \frac{10^{22} T^{7/2}}{zN^2} \times \begin{cases} 480 z^{-2}, \\ 1.3 (z^2 + z)^{-1}, \\ 4.4 (1 + z)^{-2}, \end{cases} \quad (2.4)$$

applicable, respectively, to the absorption mechanisms involving free-free transitions, to substances with one ionization-type absorption level (as found in the case of lithium), and to media with multiply ionized atoms. In the case of an optically opaque plasma, the radiation flux is

$$S = -\frac{16}{3} \hat{\sigma} T^3 l_R \nabla T, \quad (2.5)$$

where $\hat{\sigma} = 5.67 \times 10^{-5}$ erg.cm^{-2}.deg^{-4}.sec^{-1} is the Stefan-Boltzmann constant. This limit is known as the radiative heat transfer approximation. The emission of radiation from the plasma is then of the surface type and similar to the emission of radiation from a black body.

In the opposite limit, where $l_R \gg r_0$, a discharge plasma is optically transparent and the emission is of the volume type. In the case of optically transparent media, we have[31]

$$\operatorname{div} S = 10^{-27} N^2 z \sqrt{T} \times \begin{cases} 1.5 z^2, \\ 0.3 z (1 + z) \frac{J}{\varkappa T}, \\ 2.1 (1 + z)^2 \frac{\bar{J}}{\varkappa T} \end{cases} \quad (2.6)$$

respectively, for the three mechanisms mentioned above; here J is the ionization potential of the substance with one ionization level and $\bar{J} \sim \varkappa T$ (see [31]) is the average ionization potential of multiply ionized atoms.

Finally, when $l_R \sim r_0$, i.e., in the case of a semitransparent (gray) body, we must solve the system (2.3); the equations in this system cannot be simplified and, consequently, the specific mechanisms of the absorption of light in a medium are manifested most strongly in this case.

The theoretical analysis of the equilibrium, stability, and formation of light-emitting discharges was originally carried out using Eqs. (2.1)–(2.6). The numerical solutions of the various problems were often supplemented by equations describing the external circuit and by model boundary and initial conditions. However, it is more convenient to formulate these conditions separately for each specific problem.

3. Equilibrium of high-current light-emitting discharges

In investigations of the physical process in light-emitting discharges, it is usual to consider two specific variants of the discharge geometry: a simple cylindrical discharge (z or linear pinch) and a surface discharge with a reversed axial current (triaxial system or inverse pinch), shown in Figs. 1a and 1b, respectively. In this section, we shall give the results of theoretical investigations of the equilibrium of discharges of this type taking place in optically opaque, transparent, and semitransparent (gray) plasmas.

A. Equilibrium of light-emitting discharges in optically opaque plasmas. The equilibrium state of a discharge (density distribution, temperature, and magnetic field) in an optically opaque plasma is found by solving the steady-state equations (2.1), (2.2), and (2.5) for $v_0 = 0$ subject to the boundary conditions corresponding to the symmetry of the problem and the requirement of emission from the surface of a black body. However, the general form of this problem cannot be solved analytically. Fortunately, there is no need to solve the general problem in the case of discharges considered as efficient light sources. This is due to the fact that a discharge in an optically opaque plasma may be an efficient light source if the distribution of the temperature across the plasma is highly homogeneous. Subject to this assumption, the system (2.1), (2.2), and (2.5) can be solved quite easily and distributions of the equilibrium values in the case of a simple cylindrical discharge (z pinch) are given by[16,20]

$$\rho_0 = \rho_0(0)\left(1 - \frac{r^2}{r_p^2}\right), \quad P_0 = P_0(0)\left(1 - \frac{r^2}{r_p^2}\right), \quad B_0 = \sqrt{4\pi P_0(0)}\,\frac{r}{r_p},$$
$$T_0 = T_0(0)\left[1 - \frac{r^2}{r_T^2}\left(1 - \frac{r^2}{r_p^2} + \frac{r^4}{3r_p^4}\right)\right], \quad (3.1)$$

where the characteristic dimensions of the density r_p and temperature r_T in inhomogeneities are

$$r_p^2 = \frac{c^2 P_0(0)}{\pi \sigma_0^2(0) E_0^2}, \quad \frac{r_T^2}{r_p^2} = \frac{64\pi}{3} \frac{\hat{\sigma}\sigma_0(0) T_0^4(0) l_p(0)}{c^2 P_0(0)} \gg 1. \quad (3.2)$$

Here, $P_0(0)$, $T_0(0)$, $\rho_0(0)$, $\sigma_0(0)$, and $l_R(0)$ are the equilibrium values of the parameters on the discharge axis. We can easily express these parameters in terms of the total number of particles N_t in a discharge and the total discharge current I_t:

$$T_0 = \frac{I_t^2}{2(1+z)c^2 \varkappa N_t} = 3.6 \cdot 10^{13} \frac{I_t^2}{(1+z)N_t}, \quad N_0(0) = \frac{3}{2\pi}\frac{N_t}{r_p^2};$$
$$r_p = \frac{(2N_t(1+z)\varkappa c^2)^{11/6}}{\left(2\pi^2 c^2 \frac{\alpha}{z}\right)^{1/3} I_t^3} = 8.15 \cdot 10^{-21} z^{1/3} (1+z)^{11/6} \frac{N_t^{11/6}}{I_t^3}. \quad (3.3)$$

The radiation emitted by an optically opaque plasma is naturally identical with the radiation emitted by the surface of an absolute black body and in the z-pinch case discussed above the total power emitted from a unit length of the discharge is

$$W = 2\pi r_p \hat{\sigma} T_0^4 = \frac{2\pi\hat{\sigma} I_t^4}{[2(1+z)c^2 \varkappa N_t]^{13/6} (2\pi^2 c^2 \alpha/z)^{1/3}} = \frac{5.1 \cdot 10^{23} z^{1/3} I_t^4}{(1+z)^{13/6} I_t^{13/6}}. \quad (3.4)$$

The area of the emitting surface and, therefore, the total radiation power per unit length of the discharge can be increased conveniently by employing an inverse pinch as the light source. The equilibrium of light-emitting discharges of this type has been considered in several papers[14-16,18,19] and it has been found that the outer radius of the surface discharge to its thickness should be selected by varying the reverse current. In particular, when the reverse current is close to half the forward discharge current, the outer radius of the discharge

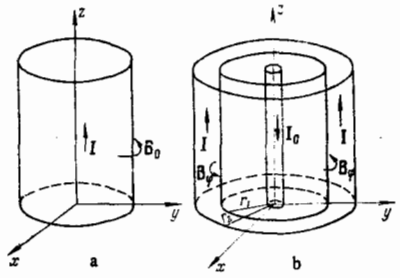

FIG. 1.

is much greater than its thickness and the discharge is of a quasiplanar surface nature. The steady-state equations (2.1), (2.2), and (2.5) for the distribution of equilibrium quantities in the inverse pinch in an optically opaque plasma yield

$$\rho_0=\rho_m\left(1-\frac{x^2}{x_p^2}\right),\quad P_0=P_m\left(1-\frac{x^2}{x_p^2}\right),\quad B_0=\sqrt{8\pi P_m}\,\frac{x}{x_p},$$
$$T_0=T_m\left[1-\frac{x^2}{x_T^2}\left(1-\frac{x^2}{x_p^2}+\frac{x^4}{3x_p^4}\right)\right], \tag{3.5}$$

where

$$x_p=\frac{c^2P_m}{2\pi\sigma_m^2E_\theta^2},\quad \frac{x_T^2}{x_p^2}=\frac{64\pi\sigma_m\hat{\sigma}_mT_m^4l_m}{3c^2P_m}\gg 1, \tag{3.6}$$

ρ_m, P_m, T_m, σ_m, and l_m are the equilibrium values of the equilibrium quantities at the maximum-density point, i.e., at $x=0$. As in the case of the z pinch, we can easily represent these quantities in terms of the total number of particles in a discharge, forward (or reverse) current, and outer radius of the discharge:

$$T_m=\frac{2\cdot10^{-2}z^{2/13}I_t^{8/13}}{R_0^{6/13}[(1+z)N_t]^{2/13}},\quad P_m=\frac{I_\theta^2}{2\pi c^2R_0^2},$$
$$x_p=7.3\cdot10^3\frac{((1+z)N_t)^{11/13}z^{2/13}R_0^{7/13}}{I_t^{18/13}}, \tag{3.7}$$

where $2I_0=I_t$.

At a given temperature, the radiation emitted from a unit length of an inverse pinch is R_0/r_p times greater than for a simple z pinch. However, the main advantage of an inverse pinch is that (as shown below) it is also R_0/r_p times more stable than a z pinch. Therefore, not only the power but also the duration of the emission can be varied within wide limits in the reverse pinch.

We shall now consider briefly the conditions of validity of the approximation discussed above. These conditions are represented by the inequalities $r_T\approx x_T \gg r_p\approx x_p\gg l_p$, which impose fairly rigid restrictions on the total discharge current in the case of the z pinch. In fact, for the absorption mechanism discussed in connection with Eq. (2.4), we have[21]

$$\left.\begin{aligned}&1.4\cdot10^6\frac{1+z}{z}\,(\text{A})\\&1.3\cdot10^5\frac{1+z}{z}\,(\text{A})\\&1.3\cdot10^5\qquad(\text{A})\end{aligned}\right\}=I_{\min}<I_t<I_{\max}=\left\{\begin{aligned}&4.3\cdot10^6\frac{1+z}{z}\,(\text{A}),\\&4.2\cdot10^5\frac{1+z}{z}\,(\text{A}),\\&4.2\cdot10^5\qquad(\text{A}).\end{aligned}\right. \tag{3.8}$$

When the current is $I_t>I_{max}$ and the total number of particles in a discharge N_t is fixed, the temperature distribution becomes inhomogeneous and the efficiency of a discharge as a light source decreases. At low currents, $I_t<I_{max}$, the opaqueness condition is obeyed: the discharge plasma becomes gray and, in the limit, $l_R\gg r_p$ (this is possible only if $I_t<I_{min}$) the plasma becomes optically transparent.

A similar although, in a sense, converse situation occurs in the case of an inverse pinch, which must satisfy the inequalities[18]

$$\left.\begin{aligned}&2.15\cdot10^{-43}\frac{z^3}{(1+z)^{4/10}}\frac{N_t^{22/10}}{R_0^{12/10}}\,(\text{A}),\\&4.8\cdot10^{-40}z^{17/10}(1+z)^{9/10}\frac{N_t^{22/10}}{R_0^{12/10}}\,(\text{A}),\\&1.0\cdot10^{-40}z^{4/10}(1+z)^{22/10}\frac{N_t^{22/10}}{R_0^{12/10}}\,(\text{A}),\end{aligned}\right\} \tag{3.9}$$
$$=I_{\min}<I_t<I_{\max}=\left\{\begin{aligned}&\frac{3.45\cdot10^{-42}z^3N_t^{22/10}}{(1+z)^{4/10}R_0^{12/10}}\,(\text{A}),\\&7.6\cdot10^{-39}z^{17/10}(1+z)^{9/10}\frac{N_t^{22/10}}{R_0^{12/10}}\,(\text{A}),\\&1.55\cdot10^{-39}z^{4/10}(1+z)^{22/10}\frac{N_t^{22/10}}{R_0^{12/10}}\,(\text{A}).\end{aligned}\right.$$

In this case, the condition of opaqueness of the plasma is disobeyed in the case of high currents $I_t>I_{max}$, whereas in the $I_t<I_{min}$ range the temperature distribution in the discharge becomes inhomogeneous although the plasma remains optically opaque (black).

It follows from this discussion that in the inverse pinch the dependences of the temperature and characteristic dimensions of the discharge on the external parameters (discharge current and total number of particles in the discharge) are weaker than in the linear pinch. Consequently, the range of currents in which the inverse pinch can exist is wider and the dependences of the optical thickness on the discharge current are different in the two cases. In the inverse pinch we have $\tau\propto x_p/l_R\propto I_t^{-10/13}$, i.e., the optical thickness decreases with increasing I_t, whereas in the linear discharge we have $\tau\propto I_t^2$, i.e., the optical density rises rapidly with the discharge current. This explains why the condition of optical opaqueness is disobeyed in the linear pinch at low discharge currents and in the inverse pinch at high currents. The change in the range of conditions corresponding to uniform temperature distributions in the inverse discharge, compared with the linear charge, can be explained in a similar manner.

B. Equilibrium of light-emitting discharges in optically transparent plasmas. In the case of sources of radiation of relatively long wavelengths, the energy considerations favor the use of high-current discharges in an optically transparent plasma in which the mean free path of photons is greater than the characteristic linear dimensions of the system. In such discharges, the plasma temperature is somewhat higher than in the opaque case but it is still sufficiently low to ignore the electronic heat conduction compared with the radiant energy flux (2.6). The steady-state equations (2.1), (2.2), and (2.6), governing the equilibrium of a discharge in an optically transparent plasma, can be solved analytically only in the case of a pure bremsstrahlung mechanism of light absorption and for a gas with multiply ionized atoms. In the case of substances with one ionization absorption level (as in the case of lithium), these hydrodynamic equations do not have an analytic solution; nevertheless, the analysis given below is still basically valid.

The distribution of the equilibrium quantities in a simple cylindrical discharge in an optically transparent plasma is described by the following relationships[14,15] (see also [16,20,21]):

$$P_0=\frac{P_0(0)}{[1+(r^2/r_0^2)]^2},\quad T_0=\frac{T_0(0)}{[1+(r^2/r_0^2)]^{4/3}},\quad B_0=8\pi P_0(0)\frac{r/r_0}{1+(r^2/r_0^2)}, \tag{3.10}$$

where r_0 is the characteristic radius of the discharge:

$$r_0=\sqrt{\frac{2}{\pi P_0(0)}\frac{c^2\varkappa^2(1+z)^2}{z^2\alpha\gamma}}, \tag{3.11}$$

$\gamma = 1.5\times10^{-27}$ and $\gamma = 1.5\times10^{-26}(1+1/z)^2$, respectively, for the bremsstrahlung mechanism of absorption and for a gas with multiply ionized atoms.

It should be noted that the distributions given by Eq. (3.10) are not normalized, i.e., the total number of particles captured by a discharge may—in accordance with Eq. (10)—diverge. However, this divergence is nonphysical and can be removed approximately by truncating the integration at $r = r_0$. In this way, we obtain [21]

$$T_0(0) = \frac{2I_t^2}{\sqrt[3]{4}\, c^2\varkappa(1+z)N_t}, \quad N_t = 3\sqrt[3]{2}\,\pi r_0^2 N_0(0). \quad (3.12)$$

The expressions (3.12) allow us to relate $T_0(0)$, $P_0(0)$, and $N_0(0)$ with the total discharge current I_t and the total number of particles N_t confined in a discharge.

A very important conclusion follows from the formulas (3.10): the total current in an optically transparent discharge is limited to [9]

$$I_t = \frac{2c^2\varkappa(1+z)}{z\sqrt{\alpha\gamma}}. \quad (3.13)$$

The numerical values of the current (3.13) for different mechanisms of the absorption of light in a plasma are, as expected, somewhat lower than I_{min} given by Eq. (3.8). This means that, in the range $I \sim I_{min}$, the discharge plasma is semitransparent and the Rosseland range of photons is of the order of the linear dimensions of the system (such a discharge is considered in the next subsection).

We shall now discuss the inverse pinch in an optically transparent plasma. Equations (2.1), (2.2), and (2.6) lead to the following distributions of the equilibrium quantities in such a discharge: [14]

$$P_0 = \frac{4P_m e^{-x/x_0}}{(1+e^{-x/x_0})^2}, \quad T_0 = T_m\left(\frac{4e^{-x/x_0}}{1+e^{-x/x_0}}\right)^{2/3}, \quad B_0 = \sqrt{8\pi P_m}\,\frac{1-e^{-x/x_0}}{1+e^{-x/x_0}}, \quad (3.14)$$

where $x_0 = r_0/4$. The distributions (3.14) represent the case when the reverse axial current is half the discharge current $I_t = 2I_0$ and, therefore, $R_0 \gg x_0$, so that the discharge is truly of the surface type.

It should be pointed out that, in contrast to the distributions given by Eq. (3.10), those described by Eq. (3.14) are normalized, i.e.,

$$N_t = \frac{4\pi^2}{\sqrt{3}}\sqrt[3]{4}\,N_m R_0 x_0, \quad I_t = 2\pi R_0 c\sqrt{\frac{2P_m}{\pi}}, \quad (3.15)$$

which allows us to express P_m, N_m, and T_m in terms of the total number of particles N_t confined in the discharge, total current I_t, and outer radius of the surface discharge R_0. In particular, we find that T_m is given by

$$T_m = \frac{\pi}{3^{1/2}2^{1/3}}\,\frac{I_t}{N_t\sqrt{\alpha\gamma}}\,\frac{1+z}{z}. \quad (3.16)$$

We shall conclude this subsection by pointing out that, according to the condition $l_R \gg x_0$, the discharge current (and, consequently, the values of the temperature T_m) should be greater, for given values of R_0, N_t, in the inverse pinch with an optically transparent plasma than in one with an opaque plasma. In fact, these currents should exceed the values of I_{max} given by Eq. (3.9). Therefore, in the range $I_t \approx I_{max}$ the plasma in an inverse pinch should be gray. We shall now consider such discharges.

C. Equilibrium of light-emitting discharges in optically semitransparent plasmas. It follows from simple physical considerations that under real conditions the radiation emitted by a discharge can never be identical with the radiation emitted by an absolute black body if only because the finite dimensions of a plasma make it transparent to photons of sufficiently short wavelengths. We can easily see also that the maximum efficiency of light-emitting discharges should correspond to $l_R \approx r_0$ and the radiation is close to the optically gray case (in the sense defined in Sec. 2). We shall show later that homogeneous temperature distributions may be established in such discharges because of the rapid radiative heat exchange via long-wavelength photons. If this assumption is made, we can integrate approximately the radiative transfer equation (2.3) for the bremsstrahlung mechanism of absorption and for the absorption by multiply ionized atoms. The flux of the radiation from the external surface of such a semitransparent discharge is described approximately by [17,18]

$$S = \hat{\sigma}T^4\xi(x_0), \quad (3.17)$$

where

$$\xi(x_0) = \frac{15}{\pi^4}\int_0^{x_0}\frac{x^3\,dx}{e^x-1} + \frac{10}{\pi^4}\,\frac{x_0^3}{e^{x_0}-1} \quad (3.18)$$

in the case of a linear z pinch and

$$\xi(x_0) \equiv \xi_1(x_0) = \frac{32}{\pi^4}\,\frac{x_0^3}{e^{x_0}-1} + \frac{15}{\pi^4}\int_0^{x_0}\frac{x^3\,dx}{e^x-1} \quad (3.19)$$

in the case of an inverse pinch, provided the radiation is reflected specularly by the inner surface of the pinch; here, $x_0 = h\nu_0/\kappa T$ is the dimensionless value of the limiting photon energy corresponding to the equality of the spectral range $l(\nu_0)$ and the characteristic dimensions of the discharge a_0 ($a_0 = r_p$ for a linear pinch and $a_0 = x_p$ for an inverse pinch), i.e., when the optical thickness of the discharge $\tau(\nu_0)$ is unity:

$$\tau(\nu_0) = \frac{a_0(\nu_0)}{l(\nu_0)} = \varkappa'_\nu(\nu_0)\,a_0(\nu_0) = 1. \quad (3.20)$$

In deriving Eqs. (3.17)–(3.19), we have assumed that if $\nu > \nu_0$ the plasma is completely transparent but if $\nu < \nu_0$ it is completely opaque. Moreover, in the case of multiple ionization, the dependence $\kappa'_\nu(\nu)$ is described by the usual expression for the spectral absorption coefficient of multiply ionized atoms obtained in the Kramers-Unsöld approximation [31] if $\nu < \nu_0$. However, if $\nu > \nu_0$, it is assumed that the absorption coefficient of multiply ionized atoms is identical with the expression for $\kappa'_\nu(\nu)$ in the case of pure bremsstrahlung mechanism of absorption but with a correction coefficient found from the requirement of continuity of $\kappa'_\nu(\nu)$ at $\nu = \nu_0$.

If we assume that the temperature distribution is reasonably homogeneous, the nature of the spatial distributions of the equilibrium values of the density, pressure, and magnetic field in an optically semitransparent discharge remains the same (irrespective of the emission mechanism) as in the case of an optically opaque discharge [see Eqs. (3.1) and (3.5)]. In fact, the temperature distribution ceases to be parabolic and is given by a polynomial of the eighth degree. If the pinch is linear, the expression for the value of $T_0(0)$, given by Eq. (3.3), still remains the same. However, the expression for r_p changes somewhat: in fact, in the case of a semitransparent or gray discharge, we have [17,21]

$$r_p^g = \frac{r_p}{\xi^{1/3}(x_0)}, \quad (3.21)$$

where r_p is given by Eq. (3.3). Using Eq. (3.21), we find that the expression for N(0) for other parameters representing a semitransparent linear discharge be-

comes different. In the case of an inverse pinch, the expressions for all the parameters of the discharge axis become different:[18]

$$x_p^g = \frac{x_p}{\xi_1(x_0)^{2/13}}, \quad T_m^g = \frac{T_m}{\xi_1(x_0)^{2/13}}, \tag{3.22}$$

where x_p and T_m are still given by the old expressions (3.7) for an opaque planar discharge. Finally, the quantity x_0 is found from the given values of I, N_t, and R_0 by graphical solution of Eq. (3.20). The necessary expressions and graphs can be found in [17,18].

It is interesting to note that the range of existence of such a pinch with a homogeneous temperature distribution is wider than in the opaque discharge case. For example, in the case of a linear discharge and the bremsstrahlung mechanism of absorption, we have

$$2 \approx x_{0\,\min} < x_0 < x_{0\,\max} \approx 12 \tag{3.23}$$

and, correspondingly (in amperes),

$$5.3 \cdot 10^5 \left(\frac{1+z}{z}\right) < I_t < 4.2 \cdot 10^6 \left(\frac{1+z}{z}\right). \tag{3.24}$$

Hence, we can see that the upper limit of the discharge current does not change, within the limits of the accuracy of the calculations, compared with the case of an optically opaque discharge [compare with Eq. (3.8)], whereas the lower limit is considerably less. This is due to the fact that a homogeneous temperature distribution in a discharge, i.e., the necessary value of the radiative thermal conductivity, can be ensured by long-wavelength photons corresponding to the range $0 < x_0 < x_{0\,\min}$.

Since in the case under consideration we have $\xi(x_{0\,\min}) = 0.4$, it follows from Eq. (3.17) that, near the lower limit of the current, the efficiency of a gray discharge increases by a factor of about 2.5 compared with an opaque discharge.

The situation is similar in the multiple ionization case. The range of existence of the inverse pinch in the gray case is considerably wider but the increase in efficiency is relatively small. The relevant estimates are given in [18].

The case of an optically semitransparent or gray discharge is encountered most frequently and includes as its limits, corresponding to $x_0 \to \infty$ and $x_0 \to 0$, the cases of completely opaque and completely transparent discharges in plasmas with homogeneous temperature distributions.

4. Stability of high-current light-emitting discharges

In this section, we shall consider the problem of the stability of the equilibrium states in the linear and inverse discharges in optically opaque, transparent, and semitransparent gray plasmas.

It is well known that a high-current self-pinched discharge is subject to many force (bending and constriction) and overheating instabilities.[8,12] The force instabilities distort the surface and shape of the discharge and the overheating instabilities split it into overheated and supercooled regions. Clearly, the development of instabilities can reduce considerably the efficiency of discharges as light sources and it can also distort their spectral characteristics. Therefore, investigations of the stability of the equilibrium state of discharges is an important and essential task.

The stability of light-emitting discharges was considered in[13-15,17,19-21,31] by the method of normal waves, using a linearized system (2.1). It was assumed that the perturbing quantities varied in space and time, in accordance with the law $f(r)e^{-i\omega t+im\varphi+ik_z z}$. The perturbations with $m = 0$ and $k_z \neq 0$ were assumed to correspond to constrictions in a discharge, those with $m \neq 0$ and $k_z \neq 0$ to bending of the discharge, and those with $m = 0$ and $k_z = 0$ to the overheating instabilities.

A. Force instabilities in a high-current discharge of finite conductivity. We shall begin with the results applicable to an optically opaque discharge[13] (see also [16,19,21]). An analysis shows that a linear high-current discharge in an optically opaque plasma is characterized by a wide spectrum of constriction instabilities of which the most dangerous is the long-wavelength ($|k_z r_p| \ll 1$) fundamental mode ($n = 0$, where n is the number of the radial oscillation mode) with an increment given by the expression

$$\gamma \approx \sqrt{|k_z r_p|}\,\frac{v_s}{r_p} < \frac{v_s}{r_p}. \tag{4.1}$$

This increment is independent of the conductivity and equal to the increment in the case of a perfectly conducting plasma.[8,12] On the other hand, the volume oscillation modes ($n \gtrsim 1$) grow more slowly and their increment decreases with increasing conductivity, owing to the diffusion of the magnetic field of the perturbations. The increment of the volume oscillations also decreases with increasing number n. Thus, a discharge in a low-conductivity plasma satisfying the inequality

$$r_p \ll \frac{c^2}{4\pi\sigma_0 v_s} \tag{4.2}$$

is more stable to low-wavelength constriction perturbations than a discharge in a perfectly conducting plasma.

The same situation also occurs in the inverse pinch but there is an important difference: the increment of the long-wavelength fundamental constriction mode is

$$\gamma \approx \sqrt{|k_z R_0|}\,\frac{v_s}{R_0} \ll \frac{v_s}{R_0}, \tag{4.3}$$

i.e., it is r_p/R_0 times smaller than in the linear discharge. This is a consequence of the smaller curvature of the lines of force of the magnetic field of the current in the inverse pinch. Thus, the planar ($|x_p| \ll R_0$) discharge is much more stable to the most dangerous long-wavelength constriction perturbations than a simple z pinch.

The increment of the short-wavelength oscillations ($|k_z r_p| \gg 1$) rises with $|k_z|$ and can become much greater than the reciprocal of the hydrodynamic time, $\gamma \gg v_s/r_p$, or the increment of the long-wavelength modes. However, these oscillations are basically of the surface type, i.e., they are localized near the surface of the discharge and decrease exponentially toward its interior. Therefore, they only give rise to small-scale perturbations of the surface of the plasma and are not dangerous.

Constrictions also develop in a transparent discharge and their characteristic feature is the absence of the fundamental surface mode of the long-wavelength perturbations because the boundary of the discharge is not sharp [see Eq. (3.10)]. The spectrum of constrictions in an optically transparent low-conductivity plasma is similar to the corresponding spectrum of an opaque plasma.

For this reason and because, in the case of an optically transparent plasma, the most dangerous instability is of the overheating type [see Eq. (4.3)], we shall not consider in greater detail the force instabilities in such a discharge.

We shall now discuss the modes with $m \neq 0$ which are the flexural and helical perturbations of a self-pinched discharge. An analysis shows that the increment of the development of long-wavelength flexural perturbations with $|k_z r_p| \ll 1$ in a low-conductivity plasma is given by the expression

$$\gamma \approx \sqrt{\frac{2}{m}} |k_z v_s| \qquad (m \neq 0), \tag{4.4}$$

i.e., it is $|k_z r_p|$ times smaller than for the fundamental mode of the constriction instability [compare with Eq. (4.1)]. Short-wavelength perturbations are characterized by an increment which is independent of m and equal to the increment for the short-wavelength constriction instabilities. Thus, the flexural and helical instabilities in an optically opaque plasma are less dangerous than the constriction instabilities. In a transparent plasma, constrictions and bending should appear simultaneously. Moreover, a rigorous analysis and simple physical considerations show that the stability of an optically gray plasma to the force instabilities should be the same as that of an opaque plasma. Finally, it should be noted that the instabilities discussed here are a consequence of the departure from the force equilibrium in a discharge and are not related directly to the energy balance. However, the growth increments of the instabilities depend on equilibrium quantities such as the temperature T and particle density N and these are influenced strongly by the optical properties of a plasma.

B. Overheating instability. An optically transparent plasma may experience not only the force instabilities, which are due to departure from equality of the kinetic and magnetic pressures in the discharge and which cause oscillations of the hydrodynamic quantities, but also an instability due to temperature oscillations. This is known as the overheating instability corresponding to $m = 0$ and $k_z = 0$. The physical nature of the overheating instability is easily understood by writing the energy balance equations (2.1) approximately in the form

$$\frac{\partial NT}{\partial t} = \frac{j^2}{\sigma} - q(T) = \sigma E^2 - q(T) = 0. \tag{4.5}$$

The first term on the right-hand side of the above relationship describes the Joule heating and is proportional to $T^{3/2}$ ($j = \sigma E \propto T^{3/2}$ because the electric field has time to become homogeneous), whereas the second term represents the loss of heat from the interior because of radiation. If this loss depends on T less strongly than the first term (in the case of a transparent discharge we have $q \propto T^{1/2}$), the rise of T in fluctuations is not compensated by the loss of heat from the interior and the overheating instability may develop in a discharge. It follows from Eq. (4.5) that the increment of this instability is

$$\gamma \approx \frac{j^2}{\sigma_0 P_0}. \tag{4.6}$$

This instability is not dangerous in a high-temperature pinch because $\sigma_0 \to \infty$ and the increment is small. Conversely, in light-emitting low-temperature discharges, the smallness of σ_0 can make the increment (4.6) much larger than v_s/r_p, i.e., much larger than the increment of the development of the force instabilities.

Rigorous analysis shows that the overheating instability may appear at high ($\omega \gg kv_s$) and low ($\omega \ll kv_s$) frequencies. Naturally, the low-frequency instability is not dangerous and is no interest to us because the force instabilities appear in the discharge before it can develop. The high-frequency overheating instability is possible only in a low-conductivity plasma, when

$$\frac{c^2k^2}{4\pi\sigma_0} \gg \omega \gg kv_s. \tag{4.7}$$

These equalities may no longer hold when the temperature rises in the course of the development of the instability and this stabilizes the oscillations. The inequalities (4.7) also determine the dimensions of the overheated region [this region can be found by replacing ω with Eq. (4.6)]. We can see that the upper limit of the dimensions is set by the skin effect and the lower by the hydrodynamic motion of the plasma.

The radiation emitted by a plasma q(T) may have a stabilizing or destabilizing influence on the overheating instability. Thus, in the high-frequency limit, when $\omega \gg kv_s$, the density of an oscillating plasma can be regarded as constant and the radiation has a stabilizing role if $T_0(\partial q_{s0}/\partial T_0)_{\rho_0} > 0$ and, moreover, if $T_0(\partial q_{s0}/\partial T_0)_{\rho_0} > 3q_{s0}/2$ it stabilizes completely the high-frequency overheating instability. In the reverse limit of the low-frequency overheating instability ($\omega \ll kv_s$), when the plasma pressure remains constant in the course of oscillations, the emission of radiation may result in the stabilization of the discharge, provided that

$$T_0\left(\frac{\partial q_{s0}}{\partial T_0}\right)_{P_0} = T_0\frac{\partial q_{s0}}{\partial T_0} - \rho_0\frac{\partial q_{s0}}{\partial \rho_0} > \frac{3}{2}q_{s0}.$$

We usually have $\partial q_{s0}/\partial T_0 > 0$ and, therefore, the emission of radiation stabilizes the low-frequency overheating instability less effectively than the high-frequency instability.

In the case of optically opaque and semitransparent plasmas, the development of a large-scale overheating instability is impossible because of the high radiative thermal conductivity. (When this conductivity predominates, we have $q = \operatorname{div} \mathbf{S} \propto T^{15/2}$.) However, regions of dimensions smaller than l, which is the mean free path of photons in a plasma, behave as if they were transparent and an overheating instability at wavelengths $\lambda_{max} < l$ may develop inside these regions. Therefore, in an opaque discharge such small-scale overheating instabilities develop most rapidly. The results obtained are in no way dependent on the discharge geometry and, therefore, they apply equally well to the linear z pinch and to the inverse pinch.

5. Nonequilibrium high-current discharges

It is clear that the whole analysis of the plasma stability given in the preceding section is meaningful only if the time for the establishment of a self-pinched equilibrium state of a discharge is less than the times needed for the development of the various instabilities discussed above. It is clearly necessary to study the process of the establishment of an equilibrium state.[19,20]

On the other hand, there is clearly a definite interest in quasiequilibrium characteristics and in the stability of high-current self-pinched discharges, in which the discharge current oscillates strongly because of the special nature of the experimental conditions. The

theory of such alternating current discharges is developed in [32].

A. Formation of high-current discharges. A rigorous analysis of the problem of formation of an equilibrium self-pinched state of a discharge can be carried out in the general case only by a numerical solution of the equations of magnetohydrodynamics and of the radiative transfer equation together with the current circuit equations. The methods for numerical solution of the problems in radiative magnetohydrodynamics can now be regarded as sufficiently developed[11,27-29] and their application to the problems of interest to us has been found to be highly effective.[26,27]

An approximate approach to the formation of an equilibrium state in linear and inverse discharges can be applied to an opaque plasma. This approach involves the solution of the system (2.1) subject to some simplifying assumptions. These assumptions are as follows: the temperature and electric field are transversely homogeneous in the process of formation of a discharge; the pinch takes place in a fully ionized gas and the total number of particles per unit length of the discharge remains constant; the energy balance in the discharge is governed by the equality of the ohmic evolution of heat and emission of the black body radiation from the surface. An analytic solution of Eq. (2.1) is possible in two limiting cases: one is the case of slow compression, when the characteristic current rise time T is much longer than the hydrodynamic time:

$$T \sim \left(\frac{\partial \ln I_t}{\partial t}\right)^{-1} \gg \frac{r_p}{v_s}, \tag{5.1}$$

and the other case is that of a fast compression, when the opposite inequality applies.

In the first case, the nonequilibrium solutions are in full agreement with the distributions given by the formulas (3.1) for the linear discharge case and by the formulas (3.5) for the inverse surface discharge case: the only modification necessary is the assumption that the current is a known function of time. This means that, in the course of compression, the radial density and pressure distributions remain of the quasiequilibrium type and the discharge radius at any moment is governed by the total discharge current and the total number of particles in the discharge. In this case, we can apply the stability theory developed above to the process of formulation of a discharge. This description of the compression of a discharge describes correctly the real situation only in the case of discharge currents exceeding a certain critical value when the intrinsic magnetic field of the current becomes capable of confining the plasma.

If the current rises rapidly (i.e., if the rise time is shorter than the hydrodynamic time), we can ignore the kinetic pressure compared with the magnetic pressure and assume the compression to be transversely homogeneous, which yields the following equation for the compression time:

$$\tau \approx \left(\frac{r_0^3 c \sqrt{\rho_0}}{I_0^{(n)}}\right)^{1/(1+n)} \sim \frac{r_0}{v_A}. \tag{5.2}$$

In this case, the current is assumed to vary with time, in accordance with the law $I_t(t) = I_0^{(n)} t^n$; r_0 is the initial radius; ρ_0 is the initial density in the discharge; v_A is the Alfven velocity. If the current rises linearly, Eq. (5.2) leads to a well-known result.[33] The process of rapid compression is of similar nature in the case of an inverse pinch. It is then found that the characteristic compression time under fast formation conditions is

$$\tau \sim \frac{a_0}{v_A}. \tag{5.3}$$

Hence, we obtain an important result that, in the case of an inverse discharge, the fast compression time is shorter than the time needed for the development of the most dangerous long-wavelength constriction type instabilities given by Eq. (4.3). Therefore, in contrast to the z pinch, in the inverse pinch the discharge forms first and becomes compressed and then only do the instabilities develop.

Since the current in an optically transparent discharge is fixed, it follows that the problem of formation of such a discharge cannot be solved within the framework of the assumptions made in Sec. 3B.

B. Self-pinched alternating-current discharge.[32] By an alternating-current discharge, we mean one which satisfies the inequalities

$$\frac{v_s}{r_{p0}} \ll \omega_0 \ll \frac{c^2}{4\pi\sigma_0 r_{p0}^2}, \tag{5.4}$$

where ω_0 is the frequency of the current in the external circuit. Physically, these inequalities mean that the discharge current can be regarded as varying at a high frequency compared with the hydrodynamic processes but is practically constant compared with electrodynamic processes (magnetic field diffusion and absence of the skin effect). In view of the fact that the skin-effect time is short compared with ω_0^{-1}, the magnetic field cannot follow variations in the discharge current. The oscillating quantities are the temperature and velocity in the discharge. However, since $\omega_0 \gg v_S/r_{p0}$, the plasma density should remain practically constant and, consequently, oscillations of the velocity should be small enough to be negligible. This state of the discharge is defined as a quasiequilibrium state and its characteristics can be found from the equations of the system (2.1) averaged over ω_0. It is then found that, in this case, it is meaningful to speak of a distribution of the effective values I_{eff}, E_{eff}, and B_{eff} which are defined in the usual manner in terms of the amplitudes ($I_{eff} = I/\sqrt{2}$, and so on), and in terms of the quantities $T_{eff} = \delta T_{p0}$, $P_{eff} = \delta P_{p0}$ defined on the basis of the nature of the time dependence $T_{p0}(t)$. In the case of an opaque discharge, we have

$$T_p(t) = T_{p0} \mid \sin^{4/11}\omega_0 t \mid, \tag{5.5}$$

whereas, in the case of a transparent discharge,

$$T_p(t) = T_{p0} \mid \sin \omega_0 t \mid, \tag{5.6}$$

and

$$\delta = \frac{1}{2\pi} \int_{-\pi}^{\pi} \frac{T_p(t)}{T_p(0)}\, dt.$$

It follows from Eqs. (5.5) and (5.6) that in a transparent discharge the temperature oscillates in exact correspondence with the current, whereas in the opaque case the oscillations have the same frequency ω_0 but the variation near the current maxima is considerably slower than harmonic.

The quasiequilibrium state of an alternating-current discharge is described by the same relationships as the equilibrium state of a direct-current discharge but the physical quantities must be replaced by the corresponding effective values. In particular, we can still use all the relationships obtained in Sec. 3 for the effective

parameters of the discharge expressed in terms of the total current and total number of particles in the discharge.

A quasiequilibrium alternating-current discharge is subject to the same instabilities as a direct-current discharge and the increments are obtained from the expressions given in Sec. 4 by the simple replacement of the physical quantities with their effective values. Thus, there is no significant increase in the stability of such a discharge because of the dynamic stabilization.

6. High-current discharge in a high-pressure gas

Discharges in gases at high pressures (of the order of one atmosphere or more) differ from discharges in vacuum primarily because the mass of a hot plasma in the current is not constant but rises during the discharge because of the heat conduction mechanism. The discharge occurs as follows: the breakdown of a discharge gap produces a thin hot-plasma channel which expands and generates a shock wave which travels across the unperturbed gas. The shock-wave front is followed by a heat-conduction wave which ionizes and heats the gas warmed by the shock wave. The region covered by the thermal wave represents a current filament in which the Joule heat is evolved. This current filament follows the thermal wave and expands until the pressure created by the magnetic field of the current balances the kinetic pressure of the plasma. As soon as this happens, the shock wave separates from the current filament and is damped out, whereas a rarefaction wave reduces the pressure of the gas around the filament practically to zero; thus, the discharge behaves like a self-pinched discharge in vacuum.

The theory of the initial stage of the discharge, i.e., the stage of an expanding thermal wave, was developed in [24,23] (see also [24-26]). It was assumed that the plasma was optically opaque, the skin effect was absent because of the low electrical conductivity, the magnetic pressure of the discharge current was small compared with the kinetic pressure, and the velocity of the thermal-wave front was low compared with that of sound in the thermally excited region (in this limit the velocity of the thermal-wave front was equal to the velocity of flow of the gas behind the front of the shock wave, which was regarded as weak). It was found that, subject to these assumptions, the equations of hydrodynamics with radiative heat conduction had a self-similar solution in the case of a discharge current varying with time in accordance with the power law $I = Ft^{r/2}$.[3)] We shall give the results of the self-similar theory in the special case of a linear rise of the current ($r = 2$) in air at atmospheric pressure. The discharge radius r(t), plasma temperature T(t) (this temperature has a practically homogeneous radial distribution because of the high radiative thermal conductivity), and the plasma density on the discharge axis are given by [25,26]

$$\left.\begin{aligned} r(t) &= 1{,}92\cdot 10^{4} F^{0{,}33} t^{0{,}635}\ \text{cm},\\ T(t) &= 1.05\cdot F^{0{,}34} t^{0{,}033}\ \text{eV},\\ \rho(t) &= 4{,}02\cdot 10^{-6} F^{0{,}31} t^{0{,}297}\ \text{g/cm}^3; \end{aligned}\right\} \qquad (6.1)$$

here, F is expressed in units of 10^{10} A/sec. The above expressions are obtained on the assumption that the Rosseland range in air is $l_R = 6.8\times 10^{-8} T^{4/3}\rho^{-7/4}$ cm, $\sigma = 10^{14} T^{0.4}$ sec^{-1}, and the average mass of the air ions is $M_i = 29$ atomic units.[22,36]

The range of validity of the above relationships is restricted to the time intervals[25,26]

$$\frac{3{,}5}{F^{1{,}05}} \ll t \ll \frac{17}{F^{1{,}17}}, \qquad (6.2)$$

where t is measured in microseconds. The lower limit of this inequality is set by the condition $r \ll l_R$ and the upper limit is set by the absence of the pinch effect in a discharge.

It is clear that the force instabilities cannot develop in the discharge during the expansion stage as long as the magnetic pressure can be ignored. They appear only when the pinch effect sets in. The overheating instability also cannot develop because of the optical opaqueness of the discharge.

II. EXPERIMENTAL INVESTIGATIONS OF HIGH-CURRENT LIGHT-EMITTING DISCHARGES

7. Dynamics of high-current discharges formed by electric explosions of conductors in vacuum

The phenomenon of electric explosions of conductors can be used conveniently in the generation of dense low-temperature plasmas with the parameters specified in Sec. 2 (temperature $T \approx 2$–10 eV, density of charged particles 10^{18}–10^{21} cm^{-3}). Such explosions are of physical interest from several points of view and have been studied for some time. However, attention has been mainly concentrated on the phase transitions from a metal to a liquid conductor which occur during the initial stage of the process. A detailed bibliography of investigations of this stage can be found in [37]. We shall not consider in detail the main characteristics of the initial stage but only point out that when the rate of supply of the energy is sufficiently rapid and the energy itself is sufficiently large, an electric explosion of a conductor in vacuum produces a plasma filament which contains all the particles of the conductor (see, for example, [38]).

The majority of the experiments has been carried out using capacitors as energy storage devices. The development of a discharge then depends strongly on the discharge circuit parameters: the discharge may be quasiperiodic and characterized by a weak damping (as, for example, in [21,39-45]) or it may be aperiodic (see [46-48]). In the first type of discharge, which is usually observed in explosions of sufficiently short conductors, one can achieve high rates of supply of energy to the discharge, high temperatures, and brief emission of hard radiation.[44,45] Such discharges are of no practical interest as laser pumping sources, but they may provide a convenient model for the study of the physics of high-current discharges (see Sec. 9). Matched discharges of sufficiently long duration are of greater interest from the practical point of view. Nevertheless, even in oscillatory discharges the active resistance of the discharge is self-controlled in such a way that a considerable proportion of the energy is supplied during the first half-period. This is illustrated in Fig. 2 which shows the time dependences of the energy (a) and power (b) supplied to a discharge.

The initial stage of a discharge channel, formation of peripheral arcs, nature and rate of introduction of the exploding wire material into the discharge,[37,41,42,49] etc. depend strongly on the diameter of the wire being exploded and of the material of which it is made, as well as on the rate of supply of the energy and its absolute value. Figure 3 shows typical high-speed photo-

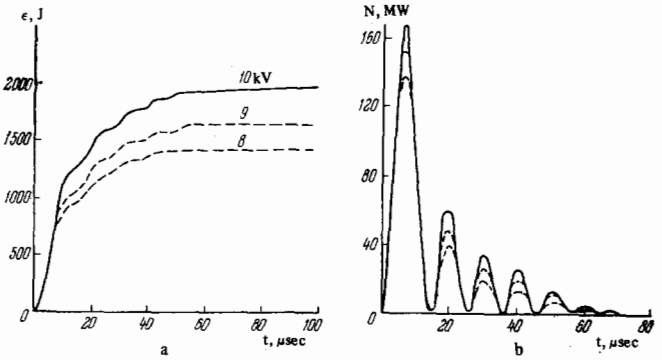

FIG. 2.

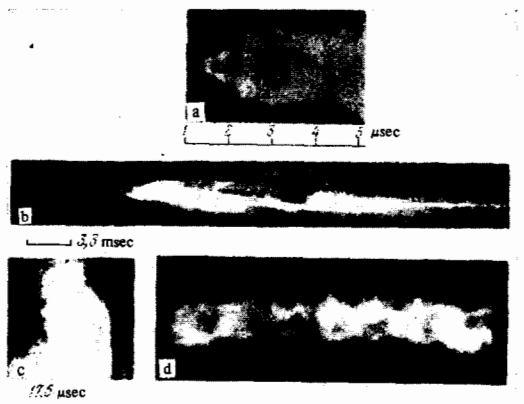

FIG. 3.

graphs (obtained with a streak camera) of discharges occurring under various conditions. Figure 3a shows a continuous time scan of the light emitted by a discharge initiated by exploding a cadmium wire of 0.1 mm in diameter in vacuum.[42] The experimental conditions were such that the discharge was quasiperiodic and the first half-period was ≈7 μsec. It is clear from Fig. 3b that the beginning of the discharge was accompanied by the appearance of intense radiation and in the early stages the radiation was emitted only from the outer shell of the wire: the discharge was peripheral with the breakdown confined to the surface (peripheral arcs are also discussed in [37,49]). Next, the radiation front expanded at a high velocity, which depended on the experimental conditions and was in the range $(1-10)\times 10^5$ cm/sec.[21,37,38,42,43,46] At the same time, the rest of the wire material was drawn into the discharge. At the moment when the current reached its maximum, all the metal vapor was inside the discharge channel. The characteristic pinch effect was also observed by this time.[38,39,42,43,47] In the case of a quasiperiodic discharge, the radiation oscillated at double the frequency of the discharge current.[43] A jet of matter ejected from the electrodes was observed in [50]. Figure 3b shows a time scan of an aperiodic discharge characterized by a relatively long first half-period (~75 μsec) which occurred in the vapor formed from a lithium wire.[46] A complex irregular structure of the discharge, typical of the situations when the rate of supply of the energy is low, was observed. Residues of the wire which retained its shape and position for a long time were observed at the center of the discharge chamber. Practically all the investigations indicated the occurrence of an instability which altered the shape of the radiation front. Typical instantaneous photographs of the discharges with instabilities are shown in Figs. 3c and 3d[46,51] (the discharge axis in Fig. 3d is horizontal).

A great variety of the spectra of the discharges produced by exploding wires was observed.[21,37-39,42-48,50,52-56] The nature of these spectra was governed by the temperature and composition of the plasma. At low densities and high temperatures the plasma was optically transparent, whereas at high densities and moderately high temperatures it was optically opaque. Since the composition and temperature of the plasma varied in the course of the development of a discharge and when the discharge current was altered, practically all the types of discharge described in Chap. I were observed in most of the experiments.

We shall now consider the main characteristics of the spectra of the discharges formed by exploding wires in vacuum, noting that, as shown in [52], the experimental results could, in many respects, depend not only on the experimental conditions but also on the technique used in recording the spectra. Figure 4 shows typical time scans of the spectra of oscillatory (Fig. 4a) and matched (Fig. 4b) discharges.[21,43,46] The spectrograms indicated that the beginning of the discharge was accompanied by an intense flash, representing a line spectrum, and this was followed by the appearance of a continuous spectrum whose intensity increased with discharge current, indicating an increase in the optical density of the plasma. The absorption lines of silicon, due to the evaporation of the walls of the discharge bulb under the action of radiation, appeared even at the early stages of the discharge. In the later stages, silicon vapor could be drawn into the discharge, giving rise to a line spectrum of the emission of the silicon ions. The later stages could also see the appearance in the discharge spectrum of the lines due to the electrode materials. In quasiperiodic discharges the variation of the spectrum with time was also periodic: repeated current maxima were accompanied by flashes producing continuous spectra with the line spectra being emitted mainly in the intervals between the flashes.

Many experiments also revealed a predischarge emission of x rays, localized near the anode,[39,44,45,53,54] whose absolute yield depended strongly on the purity of the wire. The yield of x rays was relatively smaller from a wire subjected to an outgassing process.[44] It was reported in [53] that the maximum of the x-ray power was reached at some optimal value of the plasma density (for a given voltage) and the explosion of hollow aluminum cylinders made it possible to maintain this optimal density throughout the length of the discharge. Under these conditions, x rays were emitted from the whole length of the discharge.

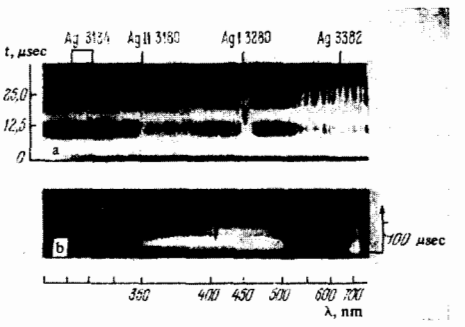

FIG. 4.

8. High-current discharge in lithium

High-current discharges, produced by exploding lithium wires in vacuum, are of special interest as sources of light,[15] have been studied in very great detail,[46,47,57-62] and are a good model of optically transparent discharges (see Sec. 3B).

A series of most detailed and systematic studies of lithium discharges was carried out at the P. N. Lebedev Physics Institute of the USSR Academy of Sciences.[46,47,57-61] The main results were obtained using apparatus in which a capacitor bank was charged to 5 kV and discharged. The first half-period was ≈75 μsec. The investigations were concentrated on discharges 14.5 cm long; the maximum current during the first half-period was 220 kA. Discharges of 92 cm in length were described in [47].

A characteristic feature of the lithium discharges was a typical turbulent structure manifested by the presence of irregular brighter bunches and helical rapidly expanding jets and by indefinite boundaries of a plasma filament expanding at a velocity of $\sim 1.3\times10^5$ cm/sec (Fig. 3b). Extended discharges (92 cm long) usually consisted of a sequence of helically twisted darker and brighter regions and the diameters of the darker regions were twice as large as those of the brighter. A similar "chain" structure was observed in [63] by exploding silver wires. This discharge structure indicated a relatively high optical transparency, confirmed by direct measurements of the optical thickness [46,47] and by the nature of the emission spectrum of the discharge.[46,58]

A time scan of the spectrum of a lithium discharge is shown in Fig. 4b. We can see that a continuous spectrum was emitted mainly at the moment when the current reached its maximum value. The Li I line was not observed in the spectrum, which indicated that the plasma was completely ionized. It was reported in [62] that when the rate of supply of the energy to a lithium wire was high but the absolute value of the energy was low, the degree of ionization of the plasma at the current maximum, found by direct measurements of the electron density from the Stark broadening of the lines, did not exceed 30%. Figure 5 shows the distribution of the spectral brightness B_ν for a bright plasma bunch. Curve 1 was obtained by exploding a wire of 0.1 mm diameter and curve 2 by exploding a wire of 0.3 mm diameter. We plotted the Planck isotherms as a series of smooth curves. We found that at wavelengths $\lambda > 4650$ Å the discharge spectrum was close to the emission spectrum of a black body at temperatures of ≈20 000°K and ≈25 000°K for the two wires, respectively. In the $\lambda < 4650$ Å range the brightness temperature fell with decreasing wavelength and the rate of fall increased with decreasing wire diameter, and, consequently, with decreasing charged particle concentration. This nature of the spectrum was in full agreement with the theoretical representations. Since the rate of expansion of the discharge channel was much less than the velocity of sound, the channel could be regarded as self-pinched and could be described by the expressions derived in Sec. 3. Since the plasma was completely ionized, we could assume that the ionic charge was $z = 1$ and this gave us $I_{min} = 260$ kA, deduced using Eq. (3.8). Thus, under the experimental conditions, the discharge as a whole should be optically transparent and should approach the optically gray state near the current maximum $I = 220$ kA.

An investigation of the yield of the vacuum ultraviolet radiation was reported in [58]. The results (Fig. 6) indicated that the radiation maximum was located at photon energies of ~2 eV and at higher energies the radiation yield fell strongly.

A relatively low density and temperature of a plasma and considerable transverse dimensions of a discharge reported in [57,59] made it possible to study the radial distribution of the main parameters of the discharge. In this way, it was possible to determine the pressure distribution (Fig. 7) as well as the distributions of the temperature and the concentration of charged particles (Fig. 8). The curves plotted in Fig. 7 were obtained by measuring the distribution of the magnetic pressure with magnetic probes (the magnetic and hydrodynamic pressures were assumed to be equal) and the points were deduced from direct measurements carried out using pressure probes.[58] The curves in Fig. 8 were obtained by measuring the distribution of the conductivity with magnetic probes and the points were deduced from the measurements of P(r) and of the optical thickness of the discharge, the results being normalized at the point r = 3 cm. The distributions of the charged particle concentration were obtained from the distributions of P(r) and T(r). In the case of a thin wire, the inhomogeneity of the temperature distribution was practically the same as that of the charged-particle distribution and, as reported, it was described satisfactorily by the relationships (3.10) applicable to a

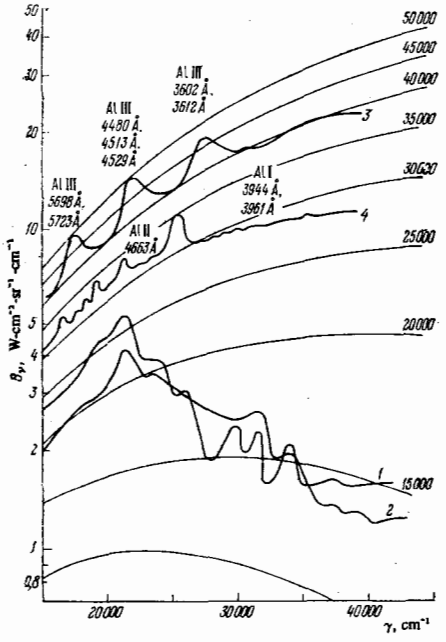

FIG. 5.

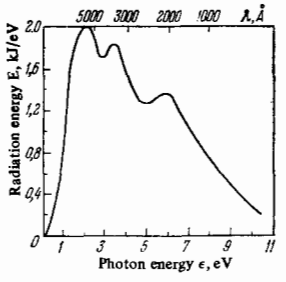

FIG. 6.

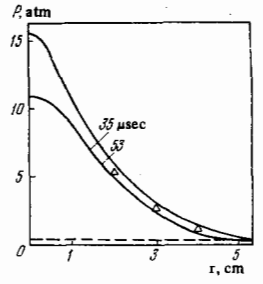

FIG. 7.

steady-state optically transparent z pinch. The distribution N(r) was more uniform in the case of thicker wires. Figure 8 also includes, for the sake of comparison, the distributions obtained by exploding an indium wire. It is worth nothing the presence of a constant-temperature region at the periphery of the discharge, indicating that the radiation emitted from this region was of the equilibrium type.

The dependences of the temperature and discharge radius on the total initial number of particles per unit length of the wire were also obtained (curves 3–6 in Fig. 9). It was found that in the case of a lithium discharge both T and r depended weakly on N_t and in the range $N_t > 4\times10^{19}$ cm^{-1} the experimental results were in satisfactory agreement with the theory [64] (dashed curve). At low values of N_t the discrepancies were large and this was attributed to the filamentary turbulent structure of the discharge.[46,61]

9. Equilibrium characteristics of optically opaque discharges

Investigations of the characteristics of the equilibrium state of optically opaque discharges were reported in[21,42,43,48]. These investigations were concerned with discharges resulting from the vacuum explosion of relatively short conductors which were mainly heavy elements. The discharges were quasiperiodic and the pinch effect was observed clearly near the first current maximum (Fig. 3a). Moreover, as reported in [21,43,48], a discharge whose length was comparable with its diameter in the magnetic confinement stage retained its cylindrical shape for a long time without visible perturbations, which was due to the stabilizing influence of the electrodes. Naturally, under such conditions, a discharge was a convenient object for checking the theory of equilibrium of self-pinched discharges. Figure 10 gives the dependence of the visible radius of a discharge on the current in the case of exploding silver wires of 0.1 mm diameter (points), which was deduced from an analysis of the patterns recorded with a streak camera. The same figure gives also the theoretical dependence deduced from Eq. (3.3) for an optically opaque discharge. The calculations were carried out on the assumption of the complete capture of the wire particles into the discharge and the value of z was calculated in accordance with the standard Kramers-Unsöld procedure.[31] We can see that the agreement is good.

The blackness of the radiation was carefully checked by an analysis of the time scans of the discharge spectra of the type shown in Fig. 4a. The spectrograms obtained indicated that an intensive continuous spectrum was emitted near the first current maximum. This continuous spectrum was used to determine the brightness temperature of the discharge T, which represented the true temperature of the discharge surface in the case of black-body radiation. The distributions of the spectral density obtained in [48,42] (see curves 3 and 4 in Fig. 5) indicated that the radiation emitted by such a discharge near the current maximum was indeed close to that expected for an absolute black body. The same curves also indicated that the degree of ionization of the plasma was high. This was particularly clear from curve 4 in Fig. 5, which indicated the presence of characteristic lines of the doubly ionized aluminum. The time dependence of the blackness temperature deduced from these data (actually, it was the dependence on the discharge current) is represented by the continuous curves in Fig. 11 (silver wire of 0.1 mm in diameter). Figure 11a was obtained for a discharge current of 160 kA at the first maximum and Fig. 11b for a corresponding discharge current of 380 kA. It is clear from Fig. 11 that the temperature followed the changes in the discharge current, reaching 2.5–5 eV at the current maximum. A similar temperature dependence was deduced from the data on the radiation yield in various spectral intervals, obtained using photocells and filters.[48] The triangles in Fig. 11 represent the values of the temperature deduced from the conductance of the discharge gap at the moment when the current reaches its maximum. In these calculations, we used Eq. (2.2) for the conductivity of a totally ionized plasma. The higher curves in Fig. 11 were obtained by calculating the temperature in accordance with Eq. (3.3). A comparison of Figs. 11a and 11b indicated that the experimental and theoretical values of T agreed satisfactorily in the case of low discharge currents. However, in the case of high currents (≈ 380 kA) the theoretical temperatures agreed well with the experimental values deduced from the conductance but were almost twice as high as the brightness temperatures. This discrepancy was attributed to a strong radial inhomogeneity of the temperature distribution: the temperatures deduced

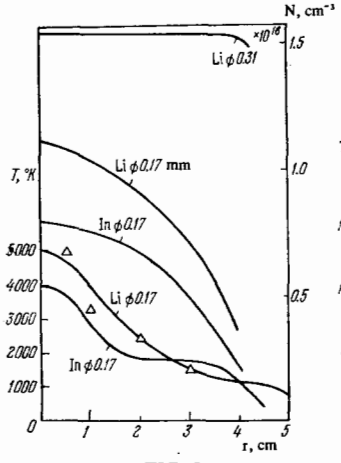

FIG. 8.

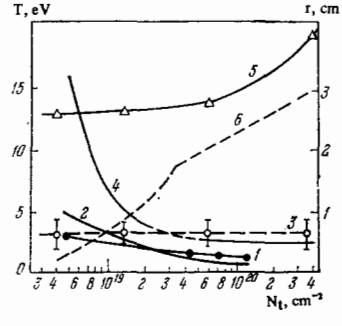

FIG. 9.

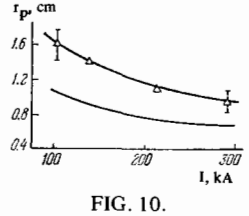

FIG. 10.

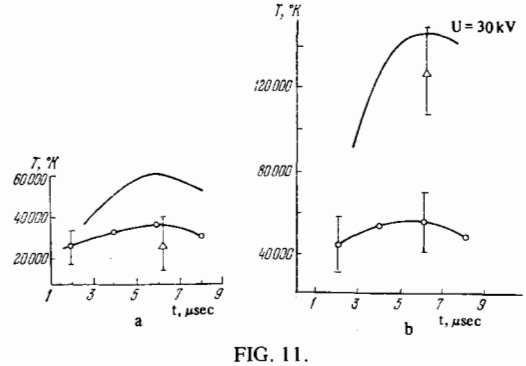

FIG. 11.

from the conductance were the average values over the cross section, whereas the brightness temperatures represented the surface of the discharge channel. The discharge current at which this discrepancy appeared was close to the theoretical value of the maximum current $I_{max} = 420$ kA [see Eq. (3.8)].

These results lead to an important conclusion. The spectrograms indicated that the radiation was black only when the discharge current was sufficiently high. This is demonstrated more clearly in Fig. 12, showing the dependence of the dimensionless brightness temperature on the wavelength, obtained for exploding aluminum, copper, silver, and tungsten wires at different moments (curve 1 corresponds to the maximum value of the current amounting to 160 kA, curve 2 corresponds to 4 μsec and a current ≈ 140 kA, and curve 3 to 2 μsec and a current of ≈ 80 kA). An analysis of such curves indicated that there was a critical value of the current below which the discharge ceased to be black and this critical value depended weakly on the material and thickness of the exploding wire, being located in the range 100–140 kA. This was in good agreement with the theoretical predictions of the existence of $I_{max} = 130$ kA. The optical thickness of the plasma was close to unity near I_{max}, as indicated by the measurements carried out using a helium-neon laser and the intrinsic radiation of the plasma. The results reported in [47] showed that in apparatus capable of producing a current of 230 kA in exploding copper and tungsten wires the emitted radiation was close to that expected for a black body of temperature 1.0–1.1 eV, whereas a lithium discharge produced a selective radiation.

The dependence of the brightness temperature on the total number of particles in a discharge is given in Fig. 9 for an opaque discharge in silver vapor (curve 1 represents the experimental results and curve 2 the theory). The discrepancy between the theory and experiment at high values of N_t is due to the partial evaporation of the wire material. The distributions of the various parameters in opaque discharges have hardly been investigated. We found in the literature only the report of an inhomogeneous temperature distribution at high discharge currents, which was mentioned above, and homogeneity of the temperature distribution in the central regions of semitransparent discharges was reported in [42].

10. Investigations of stability of high-current self-pinched discharges

The results reported in many papers [21,37,39,41,42,46-51,61,63] indicated that various types of inhomogeneity appeared in the discharges reproduced by exploding conductors in vacuum. Typical photographs of discharges with highly developed instabilities are given in Figs. 3c and 3d. The main result obtained was that the constriction and flexural instabilities developed in practically all the cases. It was established in [42] that the constrictions and helices were indeed of magnetohydrodynamic origin and the constriction instabilities were minimized by the application of an external longitudinal magnetic field. A detailed analysis of the force instabilities in an optically opaque discharge was given in [51] for discharges 25 cm long produced by exploding aluminum, copper, silver, and tungsten wires of 0.14–0.15 mm in diameter. The first half-period of the discharge was 12 μsec long and the amplitude of the current was 160 kA. Magnetic confinement appeared near the current maximum but the shape of the discharge channel was affected by strong constriction and flexural perturbations (see Fig. 3d). A spectroscopic analysis indicated the separation of various constriction and flexural modes and it was found that the maximum amplitude was exhibited by the fundamental constriction mode with $k_z r_p \approx 1$ and by the flexural instability mode with $m = 1$ and $k_z r_p \approx 0.15$. Quantitative investigations of the rate of development of the various instability modes were carried out by analyzing the time dependences of the amplitudes of these modes. The growth increments obtained in this way are plotted in Fig. 13 as a function of the atomic weight of the wire material. Curves denoted by 1 represent constrictions and those denoted by 2 represent helical instabilities. The continuous curves were obtained by theoretical calculations [see Eq. (4.1) and later expressions] and were in agreement with the experimental data. The force instabilities in transparent discharges were characterized by approximately identical increments of the constriction and helical instabilities.[45]

The development of the overheating instability in high-current self-pinched discharges has not yet been observed directly. The occurrence of a large-scale overheating instability was reported only in [65] for a wall-confined discharge in xenon. It was suggested in [46,47,58-61] that the observed structure of the discharges in lithium characterized by an irregular appearance and motion of the cold and hot regions and filaments was due to the appearance of an overheating instability in a transparent discharge. For example, it was reported in [46] that the observed discrepancies between the theoretical and experimental values of the temperature and particularly the emissivity of lithium plasmas could be explained by assuming that a discharge contained about ten overheated filaments and the diameter of each filament was ≈ 1–2 cm. However, these filaments were not observed directly. Therefore, a correlation study was made of the fluctuations of a dense lithium plasma (an analysis was made of the fluctuations of the signals picked up by magnetic probes) and these made it possible to determine the average size, fluctuation spectrum, and velocity of inhomogeneities. The average

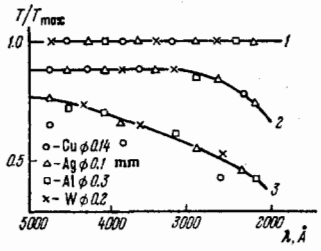

FIG. 12.

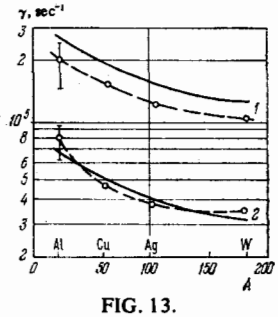

FIG. 13.

size of the plasma inhomogeneities was then found to be about 1 cm and the velocity close to the velocity of sound. A turbulent structure appeared only during the first quarter of the discharge period and then it disappeared, probably because of dissipative effects (for example, due to the emission of lines). Since an increase of the mass of the discharge (thickness of the wire) increased the optical opaqueness and reduced the turbulence in the plasma, it was concluded in [46] that the observed turbulent structure was due to the overheating mechanism.

11. Radiation yield and energy balance in discharges

The problem of the energy balance in a discharge and of the radiation yield is very important for discharges to be used as light sources. On the other hand, the solution to this problem makes it possible to provide a complete energy description and to draw the purely physical conclusions on the processes occurring in high-current light-emitting discharges.

The energy Q supplied to a discharge may represent a considerable proportion of the stored energy $\mathscr{E}$ ranging, depending on the apparatus employed, up to 60–85% for the main phase of the process.[41,46-48,63] We are primarily interested in how the energy Q is distributed in the discharge plasma. The energy of the phase transition from a metal to its vapor is usually ignored because it is relatively small. Therefore, the energy is used to ionize the gas $\sum_z N_z J_z$ (J_z is the ionization energy of an ion of charge z), to heat the gas $U = N_t \kappa T(1+z)$, to supply directional kinetic energy E_{kin}, to produce the radiation emitted from the interior $W_{\Delta\lambda_i} \equiv W_i$ ($\Delta\lambda_i$ represents the spectral interval which must be considered because the radiation is concentrated in some definite part of the spectrum), and to heat the bulb and electrodes.

Clearly, in the case of low energy inputs and short discharges, we may find that only a small proportion of the energy is converted into radiation (it was reported in [41] that only about 0.14Q was converted into radiation). In the case of a discharge gap 14.5 cm long and a quartz discharge tube of ≈9.0 cm diameter, it was found [46] that out of 17.5 kJ supplied to the discharge, the energy converted into radiation of wavelengths corresponding to the range of transparency of quartz ($\Delta\lambda_1 \approx 2200$ Å to ∞) was 6.7 kJ, the quartz tube absorbed about the same amount (6.6 kJ), and 4.3 kJ was dissipated in heating the electrodes. When the length of the discharge was increased to 100 cm, the results were quite different:[47] the energy dissipated at the electrodes remained constant, whereas the radiation energy W_1 and the energy absorbed by the discharge tube increased to 28 kJ each. It was interesting to note that W and the energy absorbed in the tube were also equal in other investigations.[48,65] The discharge tube was heated mainly by the absorption of the short-wavelength part of the radiation so that, clearly, the discharge was a very efficient converter of the electrical into the radiation energy.

In the case of discharges in the vapors of heavy elements, produced by exploding relatively thick wires, it was found that when the energy input was small, the ionization and heating of the plasma could consume a considerable proportion of the supplied energy.

In the case of discharges in the vapors of heavy elements, produced by exploding relatively thick wires, it was found that when the energy input was small, the ionization and heating of the plasma could consume a considerable proportion of the supplied energy.

It should be remembered that the relative importance of the various energy reservoirs changes in the course of a discharge. Naturally, if measurements are integrated over the whole process, the internal energy and ionization energy lose their meaning because they represent the energy lost as radiation or transferred to the walls of the enclosure or to the electrodes. If we consider the instantaneous energy balance, we may find that U and J influence strongly the state of the discharge. For example, according to the results reported in [41], the value of J up to the moment of the first maximum amounted to 45.0% of Q, and the value of U to about 25% of Q; according to the results given in [48], U + J ≈ 10% of Q. It was also interesting to note that in practically all the low-temperature self-pinched discharges the value of E_{kin} could be ignored for dense plasmas. It was generally found [46,47,48] that the value of W_1 was very close to the energy lost in the walls of the enclosure.

12. Principal characteristics of high-current discharges produced by exploding wires in dense media

The discharges initiated by electrical explosions of wires in dense gaseous media [24-26,66-79] (as a rule, in air at atmospheric pressure) can be regarded either as the transient stage of a high-power arc pulse discharge or as the early stages of spark discharges characterized by a prolonged energy input into the spark channel. In such cases, the wire may play a number of roles: in some cases, the wire material is of decisive importance[67-69] whereas, in other cases, the wire simply initiates the breakdown in long gaps caused by relatively low voltages.[22,25,26,69-79] A characteristic feature of such discharges is that they are preceded by a "current pause"[37,70-72] during which the conditions favorable for the breakdown of the gap are established in the gas surrounding the wire or in the wire vapor. The duration of this pause depends on the wire material and its diameter[37] and it increases when the density of the surrounding gas is raised. Under given conditions, the shortest pause is obtained for aluminum wires and there is practically no pause in the case of tungsten or molybdenum wires.[37,70] If the voltage is not too high, the breakdown occurs mainly on the surface of the wire.[72] The beginning of the process (the first current pulse and the associated explosive exaporation of the wire) and the secondary breakdown are accompanied by strong shock waves.[37,79] The breakdown is followed by the development of a shock wave and a simultaneous expansion of the current channel (formation of a thermal wave). The velocities of the shock and thermal waves depend on the ambient medium, rate of supply of the energy, and absolute value of the energy supplied.[22,25,26,70-75,79] In air at atmospheric pressure, the initial velocity of shock waves may reach 5×10^5 cm/sec.[75] The velocity of thermal waves is somewhat lower. A photographic scan of the explosion of a wire in air, showing clearly the first and second shock waves and the development of a thermal wave, is given in Fig. 14a. If the discharge current is sufficiently strong, the pinch effect may be observed (Fig. 14b).[25,73-75]

The discharges in air are characterized by a relatively high stability. This is demonstrated in Fig. 14c, which shows a multiframe record of a discharge in

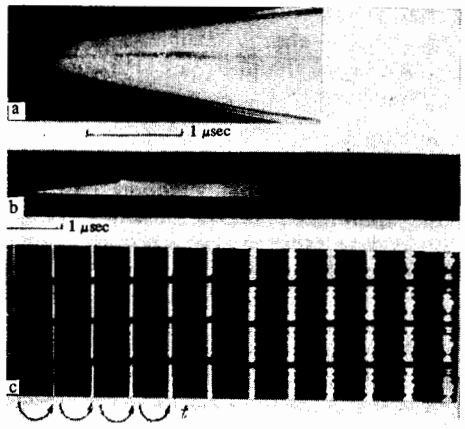

FIG. 14.

air.[26] For a long time, the discharge channel has the regular cylindrical shape with a corrugated surface. The corrugations eventually develop into clearly visible constrictions. These constrictions are particularly prominent in the pinch effect and, in this case, the rate of development of constrictions is governed (as in the vacuum pinch) by the hydrodynamic time [see Eq. (4.1)].[75]

Discharges of this type are accompanied by intensive light flashes and the radiation is basically continuous with superimposed weak emission lines typical of a given gas and wire material.[66-69,73-79] The temperature of the radiation is governed by the rate of supply of the energy and by its absolute value, as well as by the nature and pressure of the gas. If the energy is supplied rapidly, very high temperatures (up to 340 eV or higher) can be obtained.[39]

The physical processes in such discharges enable us to classify them into two groups: fast or quasiequilibrium discharges and slow or nonequilibrium discharges.

A. Fast (quasiequilibrium) discharges in air. In the case of fast discharges, the pinch effect appears in the earlier stages, when the energy supplied is only partly used up. Consequently, the range of validity of the self-similar theory [see Eq. (6.2)] is very narrow and this theory describes only a brief initial stage of the discharge.[22,25,75] The main stage is described by the theory of alternating-current discharges (see Sec. 5B), so that these discharges can be regarded as of quasi-equilibrium type. The dynamics of fast discharges was investigated most fully in [25,75]. Figure 15 shows the time dependence of the radius of a discharge channel obtained in [25]. We can see that during the initial stage the discharge channel expands at a high velocity of $\sim(4-5)\times10^5$ cm/sec and the pinch effect appears near the moment when the first current maximum is reached. The discharge channel then expands at a practically monotonic but much slower rate ($\sim5\times10^4$ cm/sec).

The radiation emitted by such a discharge is periodic with very pronounced "blackness" periods located near the maxima of the discharge current (Fig. 16a). An intense line spectrum is found to be superimposed on a continuous spectrum near the current minima. Figure 17 shows the time dependence of the brightness temperature (circles) deduced from the continuous spectrum in the blackness periods and of the temperature calculated from the conductance of the discharge near the first current maximum (triangle). The time dependence

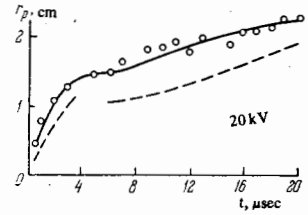

FIG. 15.

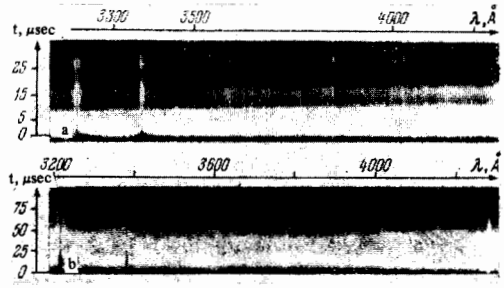

FIG. 16.

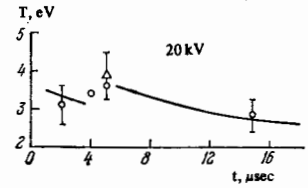

FIG. 17.

of the blackness temperature follows the corresponding dependence of the discharge current, i.e., it oscillates fairly strongly. The agreement between the brightness temperature and the temperature deduced from the conductance indicates that the temperature is distributed uniformly in the transverse direction. On the other hand, we must mention the results reported in [67-69], which indicate that the temperature decreases from the axis of the discharge. However, this applies to the later stages of the discharge, when the plasma is optically transparent so that these results cannot be used to predict the temperature distribution during the main stage of the discharge when the plasma is opaque.

Figures 15 and 17 also include the results of theoretical calculations based on the self-similar theory (initial parts of the curves) and on the theory of the alternating-current vacuum pinch beyond the first current maximum. The agreement is good, which shows that the theoretical assumptions made in Sec. 6 are correct. This description of a fast discharge (self-similar conditions during the formation of a thermal wave, pinch effect and separation of a shock wave, alternating-current discharge surrounded by a low pressure region) is also supported by the results given in [67-69] which show that the characteristics of the later stages of a fast discharge in air are governed entirely by the presence of the vapor formed from the exploded wire.

B. Slow (nonequilibrium) discharges in air. Slow nonequilibrium discharges allow us to investigate the physical processes which occur in a freely developing thermal wave and to check, over a sufficiently long time interval, the self-similar theory. They are also of direct practical interest from the point of view of energy pumping of lasers.

The principal characteristics of such slow discharges are discussed in [26,74-76,79]. The results of a high-speed photographic study of a slow discharge are shown in Figs. 14a and 14b, whereas Fig. 18 shows the time dependence of the radius of the discharge channel. The continuous curves are the experimental results (the length of the discharge was 75 cm, duration of the first half-period ~54 μsec, Nichrome wire of 0.1 mm in diameter exploded in air at atmospheric pressure). The experimental points correspond to different charging voltages U_0 and, therefore, to different rates of rise of the current $F = \dot{I}$. When U_0 is increased, the velocity of the thermal wave rises and the pinch effect tends to develop near the current maximum.

The time scan of the spectrum of this discharge, shown in Fig. 16b, demonstrates that an intense continuous spectrum is emitted during the first half-period of the current and the brightness of this spectrum rises with the discharge current. The intensity maximum coincides in time with the discharge current maximum. Similar results were also deduced from the oscillograms of signals produced by photocells which recorded the radiation emitted in narrow spectral intervals in the visible and ultraviolet range.

Figure 19 shows the time dependence of the brightness temperature deduced from the continuous spectrum during a "blackness" period (10–50 μsec); this dependence is denoted by circles. The triangle in Fig. 19 represents the temperature calculated from the conductance of the discharge. As in the case of fast discharges, the temperature rises with the current, reaching values up to 3 eV at the current maximum ($U_0 = 30$ kV).

All the experimental results obtained in the papers discussed here indicate that the energy is supplied mainly during the first half-period. Most of the radiation of a discharge is also emitted during this period (this applies particularly to the short-wavelength radiation). The energy characteristics of a $U_0 = 20$ kV discharge shown in Fig. 20 include the time dependences of the total energy input Q, total energy of the radiation of an absolute black body W ($0 < \lambda < \infty$), and energy W_2 (1860 Å $< \lambda < \infty$) emitted in the transparency band of air (lower continuous curve). This figure also gives the internal energy at the moment of the current maximum U and the ionization energy of air in a thermal wave J. The value of U is calculated assuming a theoretical particle concentration in the thermal zone $N \approx 10^{19}$ cm^{-3} deduced from the self-similar theory (a misprint made in [26] is worth noting here). It follows from these results that the energy input up to the moment when the current reaches its maximum value is $Q \approx 17$ kJ and the dissipated energy is $(W_2 + U + J) \approx 4 + 3.5 + 10$ kJ $= 17.5$ kJ, i.e., the quantitative agreement is good. Here, $W_2 = 0.23Q$, $U = 0.20Q$, and $J = 0.67Q$. A similar relationship between the internal and radiation energies has also been reported for fast discharges,[22,67] but the kinetic energy of directional motion is more important in such discharges.

In the experiments discussed here, the rise of current during the initial fairly extended stages can be regarded quite accurately as linear and the rate of rise of the current is ~10^{10} A/sec. Therefore, it follows from Eq. (6.2) that there is a wide range of conditions under which the self-similar theory is valid. The results of calculations based on this theory are represented by dashed curves in Figs. 18–20. A comparison of the calculated and experimental dependences shows that the

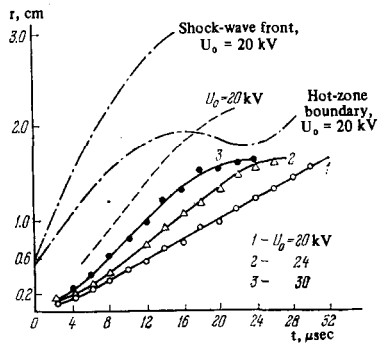

FIG. 18.

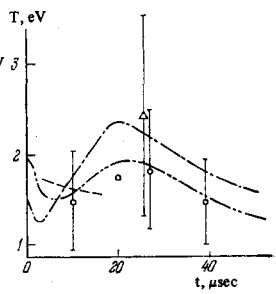

FIG. 19.

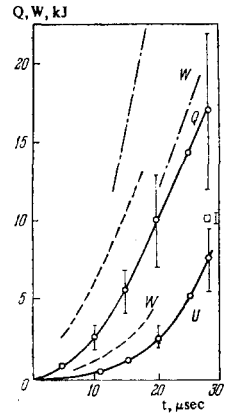

FIG. 20.

self-similar theory describes correctly the time dependences of all the quantities except the plasma temperature. However, the temperatures calculated from the self-similar theory are in good agreement with the average brightness temperatures obtained during the first half-period. Thus, the self-similar theory gives correct results in semiquantitative calculations of the principal characteristics of discharges and the precision of such calculations increases for high rates of rise of the current.

Figures 18–20 also include chain curves, which represent the discharge characteristics obtained as a result of computer solutions of the equations of radiative hydrodynamics.[26-29] These calculations were carried out using the averaged radiative transfer equation. The boundary conditions for the electromagnetic field were found using the equations for the external circuit and it was assumed that the conditions following from the symmetry of the problem were satisfied on the discharge axis. The initial state was assumed to be a cylindrical plasma column on the discharge axis (in the main variant of the calculations, it was postulated that this column had a radius $r_0 = 0.5$ cm and temperature $T_0 = 1.3$ eV). Figure 19 also includes the results of calculations of T at $r_0 = 0.8$ cm and $T_0 = 2$ eV (double-dotted chain line). These computer calculations made it possible to determine also the current-voltage characteristic of the discharge and its resistance. The results are plotted in Fig. 21 together with the experimental curves (continuous). Comparison of the curves obtained indicated that the computer calculations, made subject to the assumptions stated above, described satisfactorily the current-voltage characteristic and the variation of temperature. In the case of the other discharge parameters, the computer calculations diverged as much from the experimental results as the self-similar theory but

with one important difference that the computer calculations described all the stages of the discharge process.

13. Formation and dynamics of coaxial plasma shells

It follows from the theory that the coaxial discharges or inverse pinches have definite advantages in the form of a larger emitting surface and a higher stability than the conventional linear discharges. However, very little experimental work has been done on the coaxial discharges. The present authors are not aware of any published work on the emission from inverse pinches. Some work has been done on thermonuclear inverse pinches[80] and on xenon ribbon lamps.[81]

The formation and dynamics of coaxial discharges in air were investigated in [77,78]. The discharge was initiated by a simultaneous explosion of eight wires placed on the circumference of a circle. In this way, it was possible to produce converging, diverging, or steady-state discharges, depending on the distribution of the current inside and outside the plasma layer. Figures 22a–22c show the results of high-speed photography of such discharges viewed from the end of a discharge chamber. Figure 22d shows, on an enlarged scale, the region of interaction between two neighboring plasma channels formed by the explosion of separate wires. In the early stages of the discharge, the separate channels expanded independently of one another at a velocity of $\approx(2-3)\times10^5$ cm/sec. When these channels came into contact, they deformed but never formed a continuous coaxial shell. This behavior of the channels was probably due to the electrostatic repulsion of the diffuse space-charge layers at the boundaries of the thermal zones. Nevertheless, the radiation emitted by such a system was close to the radiation from a continuous plasma shell. Under given conditions in a discharge circuit, the temperature of a coaxial shell was less than that of a linear discharge. The temperature of a converging discharge was higher than that of a steady-state discharge and much higher than that of a diverging one.

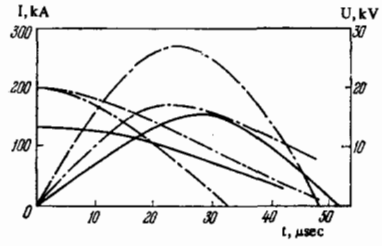

FIG. 21.

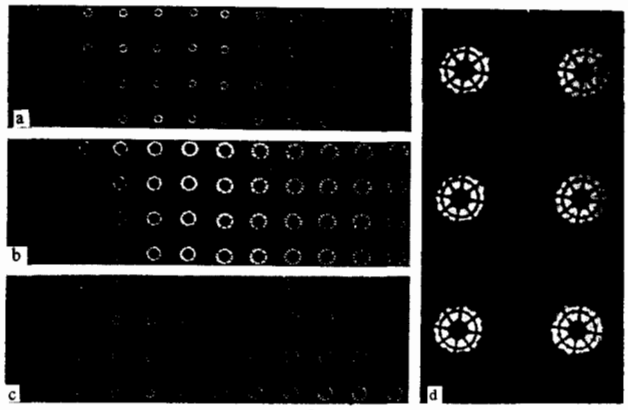

FIG. 22.

The velocity of motion of the shell toward the center of the enclosure could reach 10^5 cm/sec and this velocity increased when the rate of rise of the current was made greater. The stability of these discharges was very high and in the main stage of the process only small-scale corrugations were observed on the surface of the plasma and these were due to the initial perturbations caused by the separate wire explosions.

III. CONCLUSIONS

We shall now compare the characteristics of various types of high-current discharge considered as light sources. The main parameters of interest are the characteristic dimension of the discharge and its brightness temperature, as well as the coefficient of conversion of the supplied energy Q into the radiation energy W_i in a specified spectral range $\Delta\lambda_i$: $\eta_i = W_i/Q$. It follows from the data on the ratiation emitted from high-current discharges and on the temperature of such discharges, given in the preceding chapters, that they are distinguished by a high brightness of the emitted radiation and the capability of producing any required absolute radiation yield. Therefore, it is very important to know the conditions for attaining the optimal operation of a discharge (maximum value of η in the required spectral interval and the necessary geometrical dimensions or the velocity of propagation of a current filament). Since the discharge length and its period differ from one experiment to another, it is convenient to compare the results at some particular moment and to reduce them to a unit length of the discharge. It is convenient to consider the rate of expansion at the beginning of a discharge and temperature at the moment when the current reaches its maximum value.

Figures 23 and 24 show the dependences of the velocity of expansion v of a plasma channel and of the brightness temperature T of this channel on the energy $Q' = Q/l$ per unit length of the discharge. These dependences are plotted for a vacuum discharge resulting from the explosion of a silver wire of 0.1 mm diameter[63] and for an atmospheric discharge.[75] We can see that both v and T rise monotonically with Q′.

Figures 25 and 26 show, for the same discharges, the dependences of the specific radiation energies W_1', W_2', W_3' and of the conversion coefficients $\eta_{1,2,3}$ on Q′. It is very important to note that the values of η have maxima at some specific energy input: in atmospheric discharges this maximum is reached at $Q' \approx 0.5$ kJ/cm and in vacuum discharges it is reached at $Q \approx 0.6$–0.75 kJ/cm. This behavior is due to a redistribution of the energy supplied between the radiation and the internal energy of the discharge.

It should also be pointed out that, in the majority

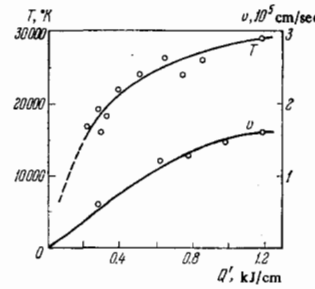

FIG. 23.

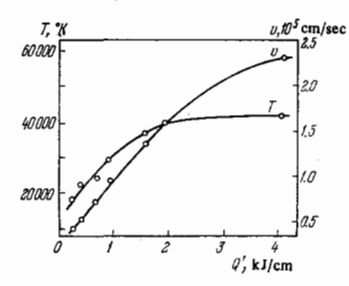

FIG. 24.

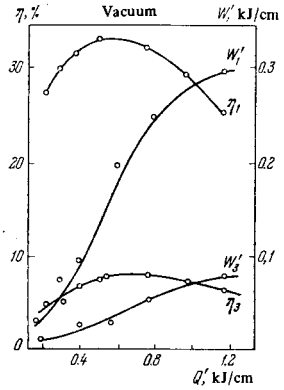

FIG. 25.

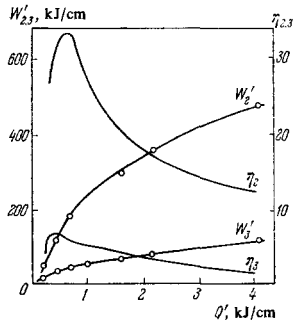

FIG. 26.

TABLE I.

Type of discharge		IFP-5000 lamp [26]	UF 900/20 lamp [26]	Explosion of lithium wire in vacuum [46,47]		Discharge in air [26,75]		Explosion of silver wire in vacuum [48,63]	
Length of discharge l, cm		25	90	14.5	92	75	75	95	95
Duration of main stage of discharge τ, μsec		620	150	70	140	55	55	—	86
Stored energy $\mathcal{E}$, kJ		5	20	26.5	72	83	225	56.7	72.3
Supplied energy Q, kJ		4	16	17.5	60	60	180	36	51
Maximum temperature T, °K		9000	110 000	17 000	28 000	26 000	31 000	21 500	24 000
Radiation energy (kJ)									
	W_1	—	—	—	28	—	—	12.5	20,5
	W_2	—	—	—	—	20	35	—	—
	W_3	0.2	1.0	1.0	—	4.4	9	2.6	2.9
Total radiation energy (quartz calorimeter), kJ		2.6	—	6.7	—	38	—	19	29
Conversion coefficient (%)	η_1	—	—	—	46.5	—	—	34.5	40
	η_2	—	—	—	—	33.4	19.5	—	—
	η_3	5	6.25	5.7	—	7,35	5	7.2	5.7

of the experiments described above, the coefficient of conversion of the stored energy $\mathcal{E}$ into the electrical energy is high: $Q=(0.7-0.8)\,\mathcal{E}$.[22,26,46-48] Calorimetric measurements indicate up to 45% of the stored energy is transformed into light and, in the case of atmospheric discharges,[26] the total radiation yield may amount to 40 kJ, which is greater than the absolute yield of any other known pump lamp.

The main data on the various types of light-emitting discharge are collected in Table I, which shows that such discharges are promising as laser pumping sources. Further improvement in the characteristics of light-emitting discharges (an increase in the stability and absolute radiation yield) may be expected from coaxial discharges (inverse pinches).

[1)] A review of the latest investigations of the high-temperature thermonuclear pinch effect, known as the plasma focus, is given in [10,11].

[2)] $[\mathbf{v}, \mathbf{B}] \equiv \mathbf{v} \times \mathbf{B}$.

[3)] The self similar solutions of the equations of hydrodynamics in the case of an optically transparent plasma (spark discharge) were obtained earlier. [34,35]

[1] I. S. Marshak, Impul'snye istochniki sveta (Pulsed Light Sources), Gosénergoizdat, M., 1963.

[2] A. F. Aleksandrov, I. S. Marshak, and A. A. Rukhadze, Zh. Tekh. Fiz. (in press) [Sov. Phys.-Tech. Phys. (in press)].

[3] W. Lochte-Holtgreven, Rep. Prog. Phys. 21, 312 (1958).

[4] M. P. Vanyukov and A. A. Mak, Usp. Fiz. Nauk 66, 301 (1958) [Sov. Fiz.-Usp. 1, 137 (1958)].

[5] M. R. Bedilov, V. P. Likhachev, V. V. Mikhaĭlov, and M. S. Rabinovich, Tr. Fiz. Inst. Akad. Nauk SSSR **32**, 97 (1966).

[6] G. K. Oster and R. A. Marcus, J. Chem. Phys. **27**, 189 (1957).

[7] W. H. Bennett, Phys. Rev. **45**, 890 (1934).

[8] L. A. Artsimovich, Upravlyaemye termoyadernye reaktsii, Fizmatgiz, M., 1961 (Controlled Thermonuclear Reactions, Gordon and Breach, New York, 1964).

[9] D. J. Rose and M. Clark, Plasmas and Controlled Fusion, MIT Press, Cambridge, Mass., 1961 (Russ. Transl., Gosatomizdat, M., 1963).

[10] N. V. Filippov. V. I. Agafonov, I. F. Belyaeva, V. V. Vikhrev, V. A. Gribkov, L. G. Golubchikov, V. F. D'yachenko, V. S. Imshennik, V. D. Ivanov, O. N. Krokhin, M. P. Moiseeva, G. V. Sklizkov, and T. I. Filippova, Proc. Fourth Conf. on Plasma Physics and Controlled Nuclear Fusion Research, Madison, USA, publ. by International Atomic Energy Agency, Vienna, 1971, p. 573.

[11] V. F. D'yachenko and V. S. Imshennik, Sb. Voprosy teorii plazmy, pod red. M. A. Leontovicha (Collection: Problems in Plasma Theory, ed. by M. A. Leontovich), Vol. 5, Atomizdat, M., 1967, p. 132.

[12] B. B. Kadomtsev, Sb. Voprosy teorii plazmy, pod red. M. A. Leontovicha (Collection: Problems in Plasma Theory, ed. by M. A. Leontovich), Vol. 2, Atomizdat, M., 1963, p. 132.

[13] A. A. Rukhadze and S. A. Triger, Zh. Prikl. Mekh. Tekh. Fiz. No. 3, 11 (1968); Zh. Eksp. Teor. Fiz. **56**, 1029 (1969) [Sov. Phys.-JETP **29**, 553 (1969)]; Zh. Tekh. Fiz. **40**, 1817 (1970) [Sov. Phys.-Tech. Phys. **15**, 1418 (1971)].

[14] V. B. Rozanov, A. A. Rukhadze, and S. A. Triger, Zh. Prikl. Mekh. Tekh. Fiz. No. 5, 18 (1968).

[15] V. B. Rozanov, Dokl. Akad. Nauk SSSR **182**, 320 (1968) [Sov. Phys.-Dokl. 13, 914 (1969)].

[16] A. F. Aleksandrov, A. A. Rukhadze, and S. A. Triger, Proc. Ninth Intern. Conf. on Phenomena in Ionized Gases, Belgrade, 1969, p. 379; Sb. Voprosy fiziki nizkotemperaturnoĭ plazmy (Collection: Problems in Physics of Low-Temperature Plasma), Nauka i Tekhnika, Minsk, 1970, p. 148.

[17] A. F. Aleksandrov, E. P. Kaminskaya, and A. A. Rukhadze, Zh. Prikl. Mekh. Tekh. Fiz. No. 1, 33 (1971).

[18] A. F. Aleksandrov and S. A. Reshetnyak, Zh. Prikl. Mekh. Tekh. Fiz. No. 2, 48 (1974).

[19] A. A. Rukhadze and S. A. Triger, Preprint No. 168, Lebedev Physics Institute, Academy of Sciences of the USSR, M., 1968.

[20] A. A. Rukhadze and S. A. Triger, Preprint No. 26, Lebedev Physics Institute, Academy of Sciences of the USSR, M., 1969.

[21] A. F. Aleksandrov, V. V. Zosimov, A. A. Rukhadze, V. I. Savoskin, and I. B. Timofeev, Preprint No. 72, Lebedev Physics Institute, Academy of Sciences of the USSR, M., 1971.

[22] N. G. Basov, B. L. Borovich, V. S. Zuev, V. B. Rozanov, and Yu. Yu. Stoĭlov, Zh. Tekh. Fiz. **40**, 805 (1970) [Sov. Phys.-Tech. Phys. **15**, 624 (1970)].

[23] V. B. Rozanov and V. L. Borovich, Kratk. Soobshch. Fiz. No. 12, 3 (1970).

[24] I. K. Fedchenko and Yu. K. Bobrov, Izv. Vyssh. Uchebn. Zaved. Energ. No. 12, 15 (1971).

[25] A. F. Aleksandrov, V. V. Zosimov, A. A. Rukhadze, V. I. Savoskin, and I. B. Timofeev, Kratk. Soobshch. Fiz. No. 8, 72 (1970).

[26]A. F. Aleksandrov, V. V. Zosimov, S. P. Kurdyumov, Yu. A. Popov, A. A. Rukhadze, and I. B. Timofeev, Zh. Eksp. Teor. Fiz. 61, 1841 (1971) [Sov. Phys.-JETP 34, 979 (1972)].
[27]P. P. Volosevich, V. Ya. Goldin, N. N. Kalitkin, Yu. P. Popov, V. B. Rosanov, A. A. Samarskiĭ, and R. N. Chetverushkin, Proc. Ninth Intern. Conf. on Phenomena in Ionized Gases, Belgrade, 1969, p. 348.
[28]V. Ya. Gol'din, D. A. Gol'dina, G. V. Danilova, N. N. Kalitkin, L. V. Kuz'mina, S. P. Kurdyumov, A. F. Nikiforov, Yu. P. Popov, V. S. Rogov, V. B. Rozanov, A. A. Samarskiĭ, B. V. Uvarov, L. S. Tsareva, and B. N. Chetverushkin, Preprint No. 36, Institute of Applied Mathematics, Academy of Sciences of the USSR, M., 1971.
[29]P. P. Volosevich, V. Ya. Gol'din, N. N. Kalitkin, S. P. Kurdyumov, Yu. P. Popov, V. B. Rozanov, A. A. Samarskiĭ, and B. N. Chetverushkin, Preprint No. 40, Institute of Applied Mathematics, Academy of Sciences of the USSR, M., 1971.
[30]V. B. Rozanov and A. A. Rukhadze, Preprint No. 132, Lebedev Physics Institute, Academy of Sciences of the USSR, M., 1969.
[31]Ya. B. Zel'dovich and Yu. P. Raĭzer, Fizika udarnykh voln i vysokotemperaturnykh gidrodinamicheskikh yavleniĭ, Fizmatgiz, M., 1963 (Physics of Shock Waves and High-Temperature Hydrodynamic Phenomena, 2 vols., Academic Press, New York, 1966–7).
[32]A. F. Aleksandrov and S. A. Reshetnyak, Zh. Prikl. Mekh. Tekh. Fiz. No. 2, 21 (1973).
[33]M. A. Leontovich and S. M. Osovets, At. Énerg. 3, 81 (1956).
[34]S. I. Drabkina, Zh. Eksp. Teor. Fiz. 21, 473 (1951).
[35]S. I. Braginskiĭ, Zh. Eksp. Teor. Fiz. 34, 1548 (1958) [Sov. Phys.-JETP 7, 1068 (1958)].
[36]N. M. Kuznetsov, Termodinamicheskie funktsii i udarnye adiabaty vozdukha pri vysokikh temperaturakh (Thermodynamic Functions and Shock Adiabats of Air at High Temperatures), Machinostroenie, M., 1965.
[37]W. G. Chace and K. K. Moore (eds.), Exploding Wires, Vol. 1 (Proc. First Conf., 1959), Vol. 2 (Proc. Second Conf., 1961), Vol. 3 (Proc. Third Conf., 1964), Plenum Press, New York, 1959, 1962, 1964.
[38]C. Aycoberry, A. Brin, F. Delobeau, and P. Veyrie, Proc. Fifth Intern. Conf. on Ionization Phenomena in Gases, Munich, 1961, Vol. 1, publ. by North-Holland, Amsterdam, 1962, p. 1052.
[39]J. Katzenstein, in: Exploding Wires, Vol. 1 (Proc. First Conf., 1959), Plenum Press, New York, 1959.
[40]E. C. Cassidy, S. W. Zimmerman, and K. K. Neumann, Rev. Sci. Instrum. 37, 210 (1966).
[41]V. I. Petrosyan, É. I. Dagman, D. S. Alekseenko, and P. A. Skripkina, Zh. Tekh. Fiz. 39, 2076 (1969) [Sov. Phys.-Tech. Phys. 14, 1560 (1970)]; V. I. Petrosyan and É. I. Dagman, Zh. Tekh. Fiz. 39, 2084 (1969) [Sov. Phys.-Tech. Phys. 14, 1567 (1970)].
[42]L. Niemeyer, Z. Naturforsch. 24a, 1707 (1969).
[43]A. F. Aleksandrov, V. V. Zosimov, A. A. Rukhadze, and V. I. Savoskin, Kratk. Soobshch. Fiz. No. 6, 58 (1970).
[44]I. Holmström, S. K. Händel, and B. Stenerhag, J. Appl. Phys. 39, 2998 (1968).
[45]B. Stenerhag, S. K. Händel, and A. Dejke, J. Appl. Phys. 41, 831 (1970).
[46]A. D. Klementov, G. V. Mikhaĭlov, F. A. Nikolaev, V. B. Rozanov, and Yu. P. Sviridenko, Teplofiz. Vys. Temp. 8, 736 (1970); Preprint No. 126, Lebedev Physics Institute, Academy of Sciences of the USSR, M., 1969.
[47]A. A. Vekhov, A. D. Klementov, F. A. Nikolaev, V. B. Rozanov, V. V. Rubtsov, and Yu. P. Sviridenko, Kratk. Soobshch. Fiz. No. 10, 53 (1970).
[48]A. F. Aleksandrov, V. V. Zosimov, A. A. Rukhadze, V. I. Savoskin, and I. B. Timofeev, III Vsesoyuznaya konferentsiya po fizike nizkotemperaturnoĭ plazmy, Kratkoe soderzhanie dokladov (Summaries of Papers presented at Third All-Union Conf. on Physics of Low-Temperature Plasma), Moscow State University, M., 1971, p. 176; Zh. Eksp. Teor. Fiz. 64, 1568 (1973) [Sov. Phys.-JETP 37, 794 (1973)].
[49]I. F. Kvartskhava, V. Bondarenko, R. D. Meladze, and K. V. Suladze, Zh. Eksp. Teor. Fiz. 31, 737 (1956) [Sov. Phys.-JETP 4, 637 (1957)].
[50]É. K. Chekalin and V. S. Shumanov, Sb. Svoĭstva gazov pri vysokikh temperaturakh (Collection: Properties of Gases at High Temperatures), Nauka, M., 1967, p. 106; Zh. Tekh. Fiz. 39, 71 (1969) [Sov. Phys.-Tech. Phys. 14, 46 (1969)].
[51]A. F. Aleksandrov, V. V. Zosimov, and I. B. Timofeev, Kratk. Soobshch. Fiz. No. 2, 25 (1972).
[52]E. C. Cassidy and S. Abramovitz, Appl. Spectrosc. 21, 360 (1967).
[53]I. M. Vitkovsky, P. P. Bey, W. R. Faust, R. Fulper, Jr., G. E. Leavitt, and J. D. Shipman, Jr., in: Exploding Wires, Vol. 2 (Proc. Second Conf., 1961), Plenum Press, New York, 1962, p. 108.
[54]I. M. Vitkovsky, Phys. Fluids 7, 612 (1964).
[55]H. Moesta and D. Breuer, Z. Instrumentenkd., 74, 260 (1966).
[56]M. J. Stevenson, W. Reuter, N. Braslau, P. P. Sorokin, and A. J. Landon, J. Appl. Phys. 34, 500 (1963).
[57]A. A. Vekhov, F. A. Nikolaev, and V. B. Rozanov, Preprint No. 79, Lebedev Physics Institute, Academy of Sciences of the USSR, M., 1971.
[58]A. D. Klementov, F. A. Nikolaev, and V. B. Rozanov, Proc. Tenth Intern. Conf. on Phenomena in Ionized Gases, Oxford, 1971, publ. by Donald Parsons, Oxford, 1971, p. 389.
[59]F. A. Nikolaev, V. B. Rozanov, and Yu. P. Sviridenko, Teplofiz. Vys. Temp. 10, 486 (1972); Preprint No. 99, Lebedev Physics Institute, Academy of Sciences of the USSR, M., 1971.
[60]F. A. Nikolaev, V. B. Rozanov, and Yu. P. Sviridenko, Kratk. Soobshch. Fiz. No. 4, 59 (1971).
[61]F. A. Nikolaev, Yu. V. Novitskiĭ, V. B. Rozanov and Yu. P. Sviridenko, Zh. Eksp. Teor. Fiz. 63, 844(1972) [Sov. Phys.-JETP 36, 444 (1973)]; Preprint No. 21, Lebedev Physics Institute, Academy of Sciences of the USSR, M., 1972.
[62]E. Oktay and D. R. Bach, J. Appl. Phys. 41, 1716 (1970).
[63]O. A. Surov, Diplomnaya rabota (Diploma Thesis), Moscow State University, 1972.
[64]V. V. Pustovalov and V. B. Rozanov, Sb. Voprosy fiziki nizkotemperaturnoĭ plazmy (Collection: Problems in Physics of Low-Temperature Plasma), Nauka i Tekhnika, Minsk, 1970, p. 123.
[65]A. N. Vasil'eva, I. A. Grishina, Yu. K. Zemtsov, V. D. Pis'mennyĭ, and A. T. Rakhimov, III Vsesoyuznaya konferentsiya po fizike nizkotemperaturnoĭ plazmy, Kratkoe soderzhanie dokladov (Summaries of Papers presented at Third All-Union Conf. on Physics of Low-Temperature Plasma), Moscow State University, M., 1971, p. 314.
[66]N. N. Sobolev, Zh. Eksp. Teor. Fiz. 17, 986 (1947).
[67]B. Ya'acobi, J. Quant. Spectrosc. Radiat. Transfer 9, 1097 (1969).
[68]B. Ya'acobi and P. Avivi, J. Phys. B 3, 405, 412 (1970).

[69]R. Krüger, Z. Angew, Phys. **25**, 282 (1968); Jena Rev. No. 1, 24 (1970).
[70]I. F. Kvartskhava, A. A. Plyutto, A. A. Chernov, and V. V. Bondarenko, Zh. Eksp. Teor. Fiz. **30**, 42 (1956) [Sov. Phys.-JETP **3**, 40 (1956)]; I. F. Kvartskhava, V. V. Bondarenko, A. A. Plyutto, and A. A. Chernov, Zh. Eksp. Teor. Fiz. **31**, 745 (1956) [Sov. Phys.-JETP **4**, 623 (1957)].
[71]K. B. Abramova, V. P. Valitskiĭ, Yu. V. Vanakurov, N. A. Zlatin, and B. P. Peregud, Dokl. Akad. Nauk SSSR 167, 778 (1966) [Sov. Phys.-Dokl. **11**, 301 (1966)].
[72]A. E. Vlastos, J. Appl. Phys. **38**, 4993 (1967); **39**, 3081 (1968).
[73]H. Bartels, P. Gansauge, and H. Kuhlmei, Proc. Fifth Intern. Conf. on Ionization Phenomena in Gases, Munich, 1961, Vol. 2, publ. by North-Holland, Amsterdam, 1962, p. 2032.
[74]A. F. Aleksandrov, V. V. Zosimov, A. A. Rukhadze, and I. B. Timofeev, III Vsesoyuznaya konferentsiya po fizike nizkotemperaturnoĭ plazmy, Kratkoe soderzhanie dokladov (Summaries of Papers presented at Third All-Union Conf. on Physics of Low-Temperature Plasma), Moscow State University, M., 1971, p. 179.
[75]I. B. Timofeev, Kandidatskaya dissertatsiya (Thesis for Candidate's Degree), Moscow State University, 1971.
[76]G. I. Kalgina, Diplomnaya rabota (Diploma Thesis), Moscow State University, 1973.
[77]A. F. Aleksandrov, A. T. Savichev, and I. V. Timofeev, Radiotekh. Elektron. **18**, 2147 (1973).
[78]A. F. Aleksandrov, V. I. Perebeĭnos, A. T. Savichev, and I. B. Timofeev, Zh. Tekh. Fiz. **44**, 65 (1974) [Sov. Phys.-Tech. Phys.-Tech. Phys. 19, 38 (1974)].
[79]A. F. Aleksandrov, V. V. Perebeĭnos, A. T. Savichev, and I. B. Timofeev, Zh. Tekh. Fiz. (in press) [Sov. Phys.-Tech. Phys. (in press)].
[80]O. A. Anderson, H. P. Furth, J. M. Stone, and R. E. Wright, Phys. Fluids **1**, 489 (1958).
[81]V. P. Kirsanov and S. V. Troshkin, Svetotekhnika No. 1, 12 (1967).

Translated by A. Tybulewicz